ELSEVIER

Journal of Structural Geology 26 (2004) 1803–1829

JOURNAL OF STRUCTURAL GEOLOGY

www.elsevier.com/locate/jsg

Activation of rift oblique and rift parallel pre-existing fabrics during extension and their effect on deformation style: examples from the rifts of Thailand

C.K. Morley[a,*], C. Haranya[c], W. Phoosongsee[c], S. Pongwapee[a,d], A. Kornsawan[c], N. Wonganan[b]

[a]*Department of Petroleum Geoscience, Univerisiti Brunei Darussalam, Tunku Link, Bandar Seri Begawan, Brunei Darussalam*
[b]*Department of Geological Sciences, Chiang Mai University, Chiang Mai, 50200, Thailand*
[c]*Unocal Thailand Ltd., 5th Floor Tower III, SCB Park Plaza, 19 Ratchadapisak Road, Chatuchak, Bangkok, 10900, Thailand*
[d]*PTTEP Siam Ltd., 10 Soonkornthosa Rd., Klong Toey, Bangkok, 10110, Thailand*

Received 21 April 2003; received in revised form 21 January 2004; accepted 18 February 2004

Available online 10 July 2004

Abstract

The Tertiary rift basins of Thailand have been previously interpreted in terms of strike-slip faulting. However, many of the trends oblique to the N–S orientation of the rift system appear to be inherited passive fabrics in the pre-rift, not active oblique strike-slip faults. Well developed N–S, NE–SW and NW–SE fabrics from Palaeozoic and Mesozoic orogenies exerted a strong influence on both Tertiary strike-slip and normal faults. Extensional fault systems are influenced in a number of ways by oblique pre-existing fabrics: these include (1) oblique orientation of faults, (2) preferred main fault and splay orientations oblique to the regional extension direction, (3) the location, geometry and style of transfer zones, and (4) fault linkage and displacement patterns. At high angles to the extension direction (about 45–50°) oblique extensional faults retain an essentially extensional, half graben character. Folds, thrusts, and inversion anticlines appear to be features associated with the compressional tips of individual and en-échelon compressional stepping-geometry, oblique extensional faults. In the Gulf of Thailand fabric inheritance from both the pre-rift section and syn-rift units has exerted an influence on the conjugate fault sets in the post-rift section. Experimental modelling has reproduced some key aspects of oblique extension, emphasising the degree of oblique opening as the major control on fault geometry and evolution. Equally, if not more important, is the number, relative strength, dip, strike, spacing, and type (pervasive or discrete) of fabric element.

Keywords: Oblique extension; Thailand; Transtension; Tertiary; Reactivation

1. Introduction

Continental rift systems tend to follow zig-zagging paths, influenced by zones of weakness in pre-rift sedimentary and crystalline rocks (e.g. McConnell, 1972; Dixon et al., 1987; Daily et al., 1989; Smith and Mosley, 1993). Such studies have shown that pre-existing fabric trends lying at angles up to 45–60° to the regional extension direction are commonly followed by extensional faults (as reviewed in Morley (1995)). Depending upon the strength and dimensions of the pre-existing fabric, oblique trends range from individual fault zones within regional extension-normal rift systems (e.g. Central Kenya; Le Turdu et al., 1999), to entire rift systems that trend oblique to the regional extension direction (e.g. Lake Rukwa; Morley et al., 1992; Ring, 1994). In recent years a number of studies, largely through experimental modelling, have sought to establish basic patterns of faults associated with oblique extension, investigating aspects such as strain partitioning, transfer zone geometries, and fault population characteristics (e.g. Withjack and Jamison, 1986; Tron and Brun, 1991; McClay and White, 1995; Bonini et al., 1997; Higgins and Harris, 1997; Keep and McClay, 1997; Clifton et al., 2000; McClay et al., 2002; Schlische et al., 2002). Experimental models use a limited variety of pre-existing weaknesses to simulate oblique extension. In these studies natural examples using regional fault patterns from the North Sea, Ethiopian rift and Gulf of Aden were compared with experimental models. However there are few published details about the natural fault-population characteristics or 3D fault geometries.

This paper illustrates activation of pre-existing fabrics

* Corresponding author. Tel.: +673-2-249001; fax: +673-2-249003.
E-mail address: chrissmorley@yahoo.co.uk (C.K. Morley).

0191-8141/$ - see front matter © 2004 Published by Elsevier Ltd.
doi:10.1016/j.jsg.2004.02.014

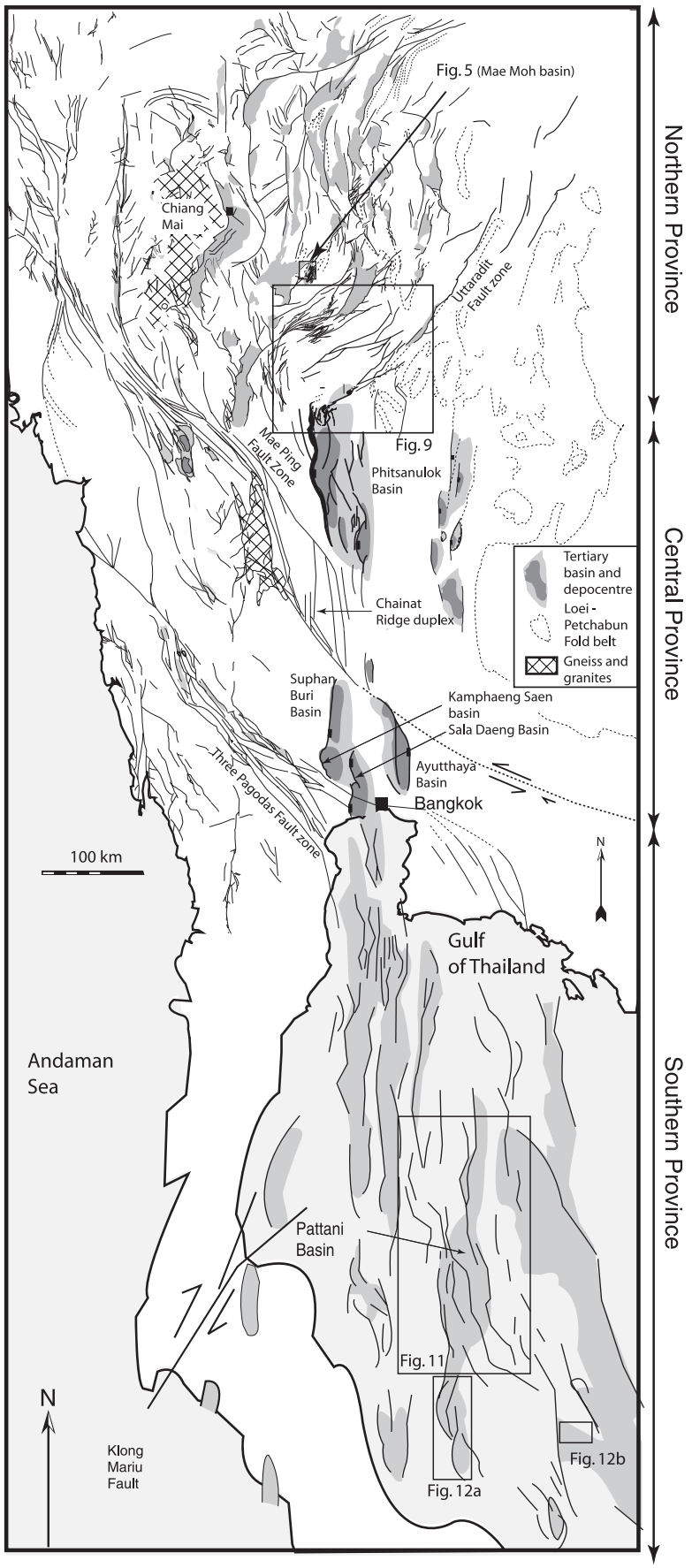
Fig. 5 (Mae Moh basin)
Chiang Mai
Uttaradit Fault zone
Mae Ping Fault Zone
Fig. 9
Phitsanulok Basin
Chainat Ridge duplex
Tertiary basin and depocentre
Loei - Petchabun Fold belt
Gneiss and granites
Suphan Buri Basin
Kamphaeng Saen basin
Sala Daeng Basin
Ayutthaya Basin
Bangkok
Three Pagodas Fault zone
100 km
N
Gulf of Thailand
Andaman Sea
Pattani Basin
Fig. 11
Fig. 12b
Fig. 12a
Klong Mariu Fault
Northern Province
Central Province
Southern Province

during extension and their effects on fault propagation and linkage geometries from natural examples, drawing on data from outcrops, open cast coal mines, satellite and seismic reflection data from Late Oligocene–Recent rift basins in Thailand (Fig. 1). Examples from northern and central Thailand show the link between basement fabrics and syn-rift structures. Offshore in the Gulf of Thailand, more complicated patterns of inheritance are present where extensive, small-displacement conjugate fault systems occur in the post-rift section. These faults formed in part due to fabrics inherited from basement and syn-rift faults and in part independently of the underlying fault systems.

2. Definition of oblique extension and transtension

One of the most widely encountered structural problems in the interpretation of rifts is determining whether the rift system evolved under an extensional or strike-slip stress regime. The Tertiary rift basins of Thailand were interpreted as pull apart basins associated with motion on NW–SE- and NE–SW-trending strike-slip faults by Tapponnier et al. (1986) and Polachan et al. (1991). These strike-slip faults are related to east and south-easterly escape of crustal blocks from the Himalayan collision zone (e.g. Leloup et al., 2001). However, Morley et al. (2000, 2001) and Rhodes et al. (2002) determined an extensional origin for the rifts and attributed many of the oblique trends affecting the large rift basins to extensional faults following pre-existing zones of weakness in the pre-rift section. They recognise some episodic motion on strike-slip faults did occur during the late Tertiary, particularly during episodes of basin inversion, and some small pull-apart basins are present particularly in the western highlands.

We use the term 'oblique extension' for activation of pre-existing fabrics striking oblique to the axis of the rift within an Andersonian stress regime for normal faults (i.e. $\sigma_1 \sim$ vertical $> ?\sigma_2 \geqq \sigma 3$). Depending upon pre-existing fabric strength, geometry, spacing and orientation, faults developed during extension may follow the pre-existing fabrics for short distances, or the faults may follow one or more oblique trends for most or all of their length. Despite the potential for strain partitioning and oblique-slip faults that may produce local non-coaxial deformation, the overall strain pattern for oblique extensional zones remains coaxial and pure shear (Fig. 2). The activation of oblique basement fabrics during extension can produce geometries somewhat similar to those produced during strike-slip (in particular, transtensional) deformation. Hence understanding the differences between the two deformation styles and their associated stress regimes is significant.

Transtension is a form of strike-slip deformation, and hence the vertical principal stress is the intermediate principal stress (Sanderson and Marchini, 1984). Conversely, for oblique extension the vertical principal stress is the maximum principal stress. Although transtension is really a stress term, it is primarily defined in terms of strain as strike-slip deformation that deviates from simple shear because of a component of extension orthogonal to the deformation zone (e.g. Sanderson and Marchini, 1984; Dewey et al., 1998; Fig. 2). Deformation is typically non-coaxial and involves strain partitioning (e.g. Fossen and Tikoff, 1993). The differences in strain pattern between oblique extension and transtension is seen in the construction of experimental models where oblique extension is produced by pure shear extension of the rig (e.g. Withjack and Jamison, 1986; Tron and Brun, 1991; McClay and White, 1995; Bonini et al., 1997; Higgins and Harris, 1997; Keep and McClay, 1997; Clifton et al., 2000; McClay et al., 2002; Schlische et al., 2002) whilst transtension is modelled by combined pure and simple shear of the rig (Schreurs and Colletta, 1998).

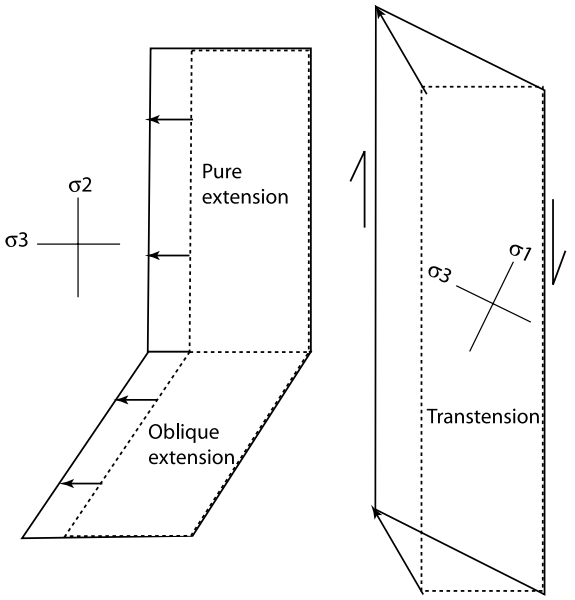

Fig. 2. Schematic plan view illustration of the differences between oblique extension (essentially pure shear) and transtension (mixed simple shear and pure shear).

3. Mechanics of oblique extension

Three main factors central to fabric reactivation at a particular scale are reviewed below: (1) strength of the fabric relative to intact rock and other fabrics, (2) the dip and strike of the fabric relative to the stress field, and (3) the sense of slip if the fabric becomes activated.

The activation of oblique fabrics during rifting can be

Fig. 1. Location map of rift basins onshore and offshore Thailand, based on the Geological Map of Thailand (Department of Mineral Resources, 2001), satellite image interpretation, field mapping and Morley (2001). Boxed areas are locations of maps presented in this paper.

split into three stages: (1) the initial fracturing of the 'intact' isotropic rock and rock with strength anisotropy during the first stages of extension, (2) subsequent activation of the established fault and fracture network, and (3) changes to the stress field (magnitude or orientation) during the evolution of the rift system.

The development of the early stage rift faults can be characterised as competition between the development of new optimally aligned fractures within isotropic rock or non-optimally aligned fractures that follow a material strength anisotropy (Fig. 3a). For a new fault to form in the theoretically ideal orientation with respect to the principal stresses the isotropic cohesive shear strength of intact country rock (C) must be overcome. The presence of discrete fabrics (e.g. cemented fault zones, shear zones, joints) or pervasive strength anisotropy (e.g. fissility, cleavage, schistosity, laminations, bedding) in the country rock affects rock strength, and reduces the cohesive shear strength (C_1) with respect to the isotropic rock strength (C) e.g. Ranalli and Yin (1990).

The potential strength anisotropy created by fabrics is considerable; commonly values of about 100 bar may be attributable to the cohesive strength of intact rock, whilst a cemented fault zone is unlikely to exceed 10 bar (e.g. Sibson, 1977). Youash (1969) demonstrated that the tensile strength of rocks loaded at 0–60° to strength anisotropic fabrics is only 25–75% to that of similar samples loaded at 90°.

The cohesive shear strength can also be defined as a continuous variable (ΔC) that changes according to the angle the plane of strength anisotropy makes with the orientation of the maximum principal stress (β) (Jaeger and Cook, 1967):

$$C_1 = \Delta C \cos 2(\alpha - \beta) \tag{1}$$

where α (the angle of shear failure with respect to σ_1, typically 30°) and β are assumed to lie between 0 and 90°. The cohesive strength is least when $\alpha = \beta$ and has a maximum value when the plane of the strength anisotropy is rotated a further 90°.

Frictional behaviour will also differ from isotropic rock strength, μ_2 is the friction angle along the strength anisotropy (coefficient of static friction), σ_{ne} = effective normal stress. Hence the Coulomb failure criteria for rock with a strength anisotropy is:

$$\tau = C_1 + \mu_2 \sigma_{ne} \tag{2}$$

Once active faults are established extensively in a rock volume the Coulomb failure criteria (which includes cohesive rock strength) is replaced by a sliding friction criteria, which is the same for almost all rock types (Byerlee, 1978). Sliding friction is controlled by the ratio and magnitude of shear stress to normal stress and is applicable under moderate to high normal stress conditions (Byerlee, 1978). Under sliding friction failure criteria, the rock strength anisotropy that allows reactivation of non-optimally oriented faults during the early stages of extension is replaced by a failure criteria for the fault zones themselves that is similar no matter what the fault orientation. In an array of faults with different orientations but similar sliding friction criteria those closest in orientation to the mechanically ideal orientations for the prevailing stress field will be favoured for reactivation (Fig. 3b). The switch in failure criteria suggests two trends in oblique fault development through time: (1) where early optimal and non-optimal faults are both present the non-optimal orientations will tend to be activated less, while optimal faults will become favoured as the rift evolves (Fig. 3b), and (2) in areas where established non-optimal faults are dominant, they will remain active if their reactivation requires differential stresses less than those necessary to initiate failure of intact, isotropic rock (Fig. 3c). Consequently domains dominated by non-optimal faults (with little early development of optimal faults) will have the greatest chance for survival throughout the rift episode.

The variation in magnitude of the intermediate principal stress value between σ_1 and σ_3 exerts an important effect on active fracture orientations (e.g. Jaeger and Cook, 1967; Carey, 1979; Angelier et al., 1982) and the orientation of the maximum shear stress, which controls the sense of fault slip (Bott, 1959). The range of strike directions of 'optimal' faults is defined by the ratio of the intermediate stress to the other principal stresses (ϕ) (Bott, 1959):

$$\phi = \frac{\sigma_2 - \sigma_3}{\sigma_1 - \sigma_3} \tag{3}$$

There is also emerging evidence from true triaxial experiments that σ_2 makes a significant impact on rock strength. The conventional triaxial tests for which $\sigma_2 = \sigma_3$ yield the lowest strength value for any given least principal stress (Chang and Haimson, 2000). As σ_2 increases, so does rock strength, to a maximum of about 50% from that determined by conventional triaxial tests (Haimson and Chang, 2000). In experiments the strengthening effect caused the fracture angle with respect to σ_3 to steepen for a fixed value of σ_3 from 55 to 75° as σ_2 was increased (Haimson and Chang, 2000).

The basic principles of fault/fabric reactivation outlined above has been integrated into software that uses material properties, stress orientation and magnitude to predict the likelihood of fault and fracture reactivation for fault seal analysis (e.g. Morris et al., 1996). The outputs from one such piece of software, the FAST program, described by Jones et al. (2000), Mildren et al. (2002) and Meyer (2002) is shown in Fig. 4. Poles to planes of all possible fault orientations are plotted with shading to define the likelihood of reactivation based on fault orientation, assuming similar strength values for all orientations. This assumption works best for the second stage of fault development when sliding friction behaviour can be assumed. The plots also help to illustrate the general principles of fabric re-activation (Fig. 4); the cases considered here are for an extensional stress

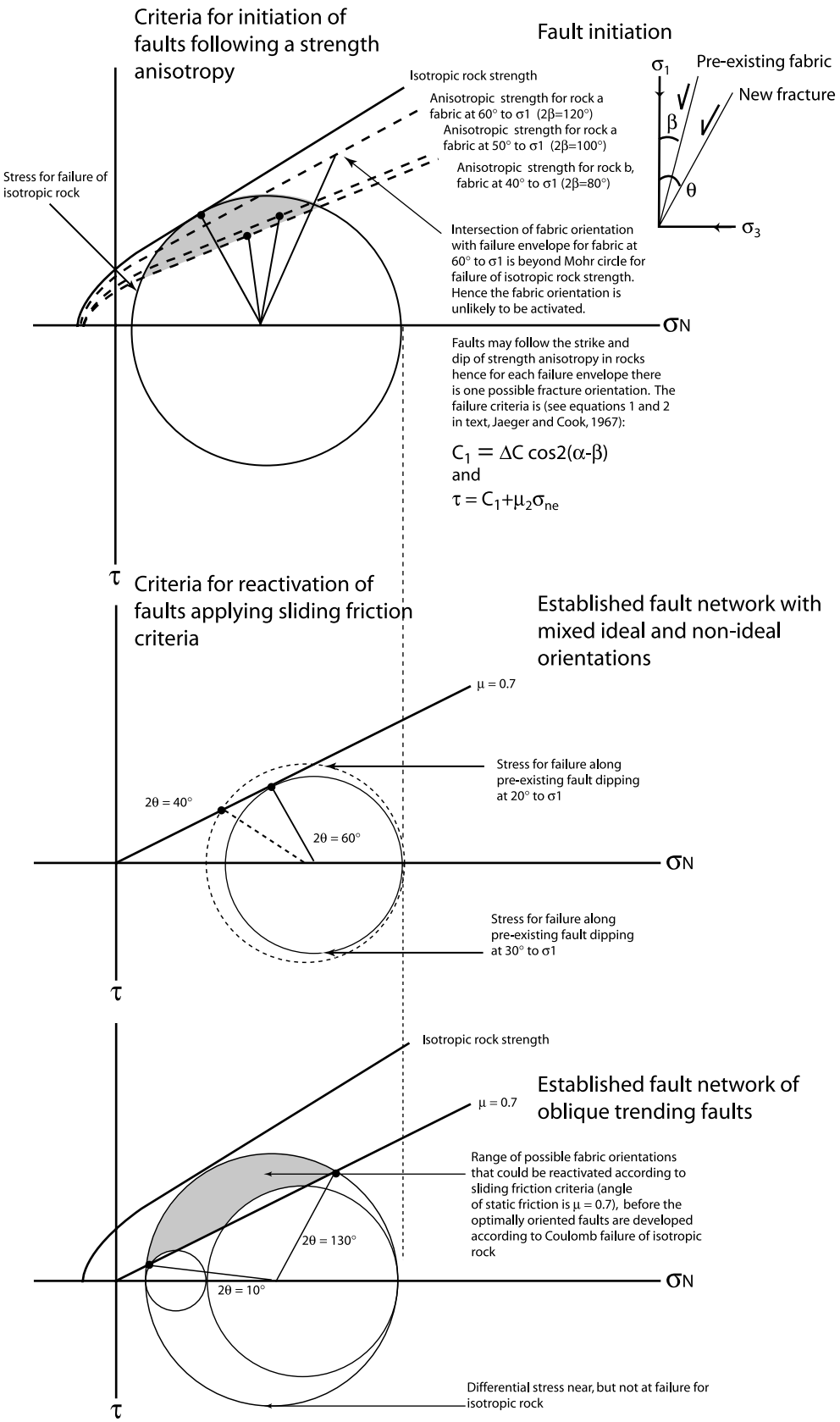

Fig. 3. Idealised Mohr circles illustrating the interplay between initiation of new optimally oriented fractures in isotropic rock, activation of oblique fabrics due to strength anisotropy and activation of cohesionless faults of optimal and non-optimal orientations.

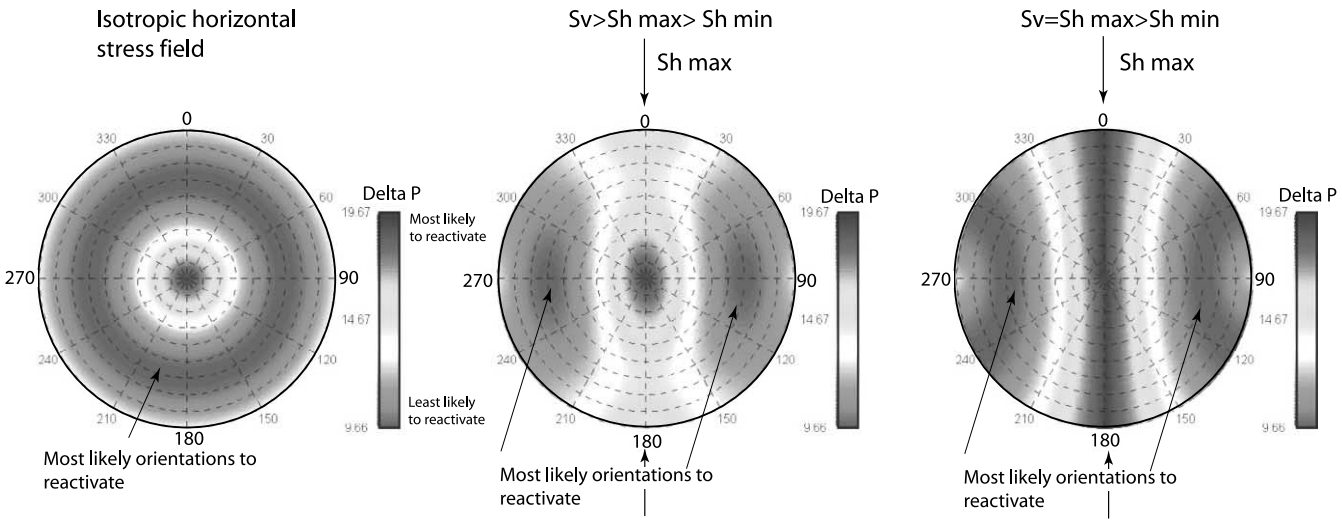

Fig. 4. Likelihood of tensile or shear failure for three cases of extensional stresses illustrating how variations in the relative magnitudes of the maximum and minimum horizontal stresses is likely to cause significant variation in the activation of weak pre-existing fabrics. Equal angle, lower hemisphere, polar stereographic projection. Coulomb failure criteria ($\mu = 0.6$), typical sedimentary basin stress tensor at 1 km depth: (a) Isotropic horizontal stress, Sv = 22.6 MPa, Sh min and Sh max = 0.7 Sv (15.8 MPa), (b) 'Pure' normal fault stress regime, intermediate Sh max of 19.2 MPa, and (c) normal/strike-slip faulting. Examples derived from FAST software (e.g. Mildren et al., 2002). This analysis is similar to the slip tendency analysis of Morris et al. (1996), but uses the change in pore fluid pressure required to cause failure (delta *P*) to measure the tendency for fault reactivation.

system. If σ_2 and σ_3 are of equal magnitude and if the fabrics are of equal strength, then any strike direction has a similar likelihood of reactivation. The main controlling factor is the dip of the anisotropy plane. As the magnitude of σ_2 increases with respect to σ_3 so the range of anisotropy orientations likely to be reactivated becomes reduced (typically to the range of 50–70° dip within 30° strike of the σ_2 axis; Fig. 4b). As σ_1 approaches σ_2 (evolving towards a more strike-slip stress regime) the range of fault orientations likely to become reactivated increases (Fig. 4c). In addition to the typical extensional fault orientations, high-angled faults oriented about 45° to σ_2 (i.e. strike-slip orientations) have a high likelihood of reactivation.

This range of anisotropy reactivation in Fig. 4 is pertinent to the rifts of Thailand because multiple phases of extension alternating with strike-slip or thrust reactivation of normal faults (inversion) have been recorded in the rift basins (Morley et al., 2000, 2001). The most likely explanation for the complex stress evolution is that Himalayan escape tectonics caused episodic variations in the magnitude (and orientation) of the NE–SW to NW–SE oriented horizontal principal stress (Huchon et al., 1994; Kong and Bird, 1996; Bott et al., 1997), and this principal stress at times of extension was σ_2 and at times of inversion was σ_1. This episodic variation may be due to a combination of factors including: changing stresses due to the northwards migration of the Himalayan syntaxis (Huchon et al., 1994), regional changes in plate boundary configuration, the activity and locking of major strike-slip faults that lay between Thailand and the Himalayas, and whether at any point in time deformation in the Himalayas favoured contractional deformation or strike-slip extrusion (Harrison et al., 1996).

4. Thailand Tertiary rift province distribution and fabric orientation

In Fig. 1 the N–S trend of rift basins of Thailand is subdivided into northern, central and southern provinces based on topography, geometry and timing of structural events. The northern area is characterised by intermontaine rift basins between hills of Mesozoic–Palaeozoic sedimentary rocks, granite intrusions and metasediments. This region is dominated by N–S to NE–SW striking Tertiary normal, oblique and strike-slip faults (Fig. 1). The NE–SW trends reflect at least in part the strike of thrusts, cleavage and foliations associated with the Indosinian Orogeny (e.g. Macdonald and Barr, 1984; Singharajwarapan and Berry, 1993; Fig. 1). Due to the young age of deformation and higher topography thermal subsidence basins are absent or poorly developed. Most geological data in the public domain comes from natural and coal mine outcrops. The regional extension direction is indicated by E–W to WNW–ESE stretching lineations on the eastern flanks of the metamorphic core complexes abutting the Chiang Mai basin (Rhodes et al., 1997), and WSW–ENE to WNW–ESE extension directions determined from fault kinematic data (Morley et al., 2000, 2001).

The central area of Thailand is a large flat region where the Tertiary rift basins are covered by a Pliocene–Recent post-rift basin. The rift basins are known through seismic reflection and well data gathered for hydrocarbon exploration. Paleogene strike-slip faults (Mae Ping and Three

Pagodas faults) have imposed a strong NW–SE fabric on parts of the area (Fig. 1; Lacassin et al., 1997). In places, individual sinistral ultramylonite shear zones are several kilometres wide (Lacassin et al., 1997), and the mapped fault zones define provinces 20–30 km wide, where large-scale slivers of mappable lithological units have NW–SE orientations (Fig. 1).

The most southerly area is offshore, where thermal subsidence began in the Oligocene–Miocene. The timing of subsidence appears to young from south to north, beginning in the Oligocene–early Miocene in the south (Morley et al., 2001). The most extensively explored basin offshore is the Pattani Basin, where widespread conjugate normal fault sets in the post-rift section form the hydrocarbon-bearing traps (Jardine, 1997; Kornsawan and Morley, 2002). Overall the region is dominated by N–S-trending faults, but, passing SE from the Pattani to the Malay basin, NW–SE fault trends become important (Fig. 1).

5. Characteristics of oblique trend activation during extension

5.1. Oblique trends in the Mae Moh mine, northern Thailand

In the model of Polachan et al. (1991) the small rift basins in Northern Thailand were formed as pull apart basins due to sinistral strike-slip motion on the NE–SW trends and dextral motion on N–S to NW–SE trends. Some of the major fault patterns around the basins swing from N–S to NE–SW trends, and could be interpreted as forming at releasing bend geometries. However the NE–SW fault trends appear to be much more discontinuous (Fig. 1) than that proposed by Polachan et al. (1991) and do not seem to have large displacements, suggesting the pull-apart model is not appropriate (Morley, 2001; Rhodes et al., 2002). The Mae Moh mine is the area where orthogonal and oblique fault patterns have been mapped in the most detail in northern Thailand.

The Mae Moh mine lies on Triassic sedimentary rocks whose bedding strikes dominantly NE–SW. These rocks in places are strongly folded, and the folds appear to be too complex, and bedding changes orientation over short distances to significantly influence fault orientation. In other places where the beds exhibit more consistent dips (around 40–70°), they may influence fault orientation, for example the large fold in Triassic rocks immediately NW of the mine (Fig. 5). Repeated, detailed mapping during open-cast mining and an extensive borehole survey prior to the initiation of mining have provided a very detailed picture of the fault pattern in the mine (Morley and Wonganan, 2000; Fig. 5). The mine exposes an area about 3 km × 4 km. The eastern part of the mine displays a simple fault pattern composed of N–S striking, overlapping, generally soft-linked faults. The western part of the mine is very different. N–S striking faults are bounded by NE–SW striking faults. The N–S striking faults have zig-zagging map patterns involving NE–SW segments. Many of the faults join or touch each other, to the point where the majority of the faults seem to be hard-linked or intersecting (Fig. 6).

In analogue models of oblique extension the degree of oblique extension (α) is defined as the angle between the oblique trend at the base of the model and the displacement direction, where 90° = pure extension and 0° = strike-slip (Withjack and Jamison, 1986). The fault pattern in the western Mae Moh mine is reminiscent of sandbox models of oblique extension with $\alpha = 45°$ (e.g. Withjack and Jamison, 1986; Tron and Brun, 1991; McClay and White, 1995; Clifton et al., 2000), and suggests that NE–SW striking oblique basement fabrics have influenced the western half of the mine, but not the eastern half. Some fault striation data was gathered from the mine (Fig. 7). Unfortunately striations were not present on the majority of faults, and the data is strongly biased towards NNE–SSW- to NE–SW-trending faults. The data shows the striations are predominantly dip-slip and tend to be oriented either parallel to the inferred E–W regional extension direction or NE–SW, i.e. pure dip-slip on oblique trends. The data are compatible with an extensional setting.

Displacements on marker horizons (especially coals) are sufficiently well constrained in the mine that the fault linkage and displacement characteristics of the normal faults can be determined (Morley and Wonganan, 2000). Sixty-five percent of eastern faults show one displacement maxima along their trace, two displacement maxima are fairly common (30%) and there was one example of three displacement maxima (Fig. 8a). The western side of the mine differs significantly, 45% of the faults show one displacement maxima, 37% show two displacement maxima, 12% show three displacement maxima, and there is one example of five. Faults with 1–2 displacement maxima tend to be the N–S trends, the faults with 3 and 5 displacement maxima follow the NE–SW trends. Faults in the western area show a wider scatter of values for displacement vs. fault length than the eastern area (Fig. 8c). This reflects the linkage of more relatively high displacement fault segments in the western area than in the eastern area. As would be expected for fault populations displaying linkage and multiple displacement maxima, the highest displacement faults in the separate western and eastern populations tend to display multiple depocentres. In the western area multiple depocentres are associated with the longest faults, which are the oblique NE–SW trends.

In the mine oblique extension has produced a much more complex pattern of fault interaction than the adjacent more pure extension region of faulting. The differences are seen in the way faults have linked and transferred displacement. Fault populations with mixed ‘ideal’ and oblique strikes must adjust to lateral barriers to propagation. Probably more ideal fault orientations (N–S) developed relatively late in the development of the fault pattern and encountered

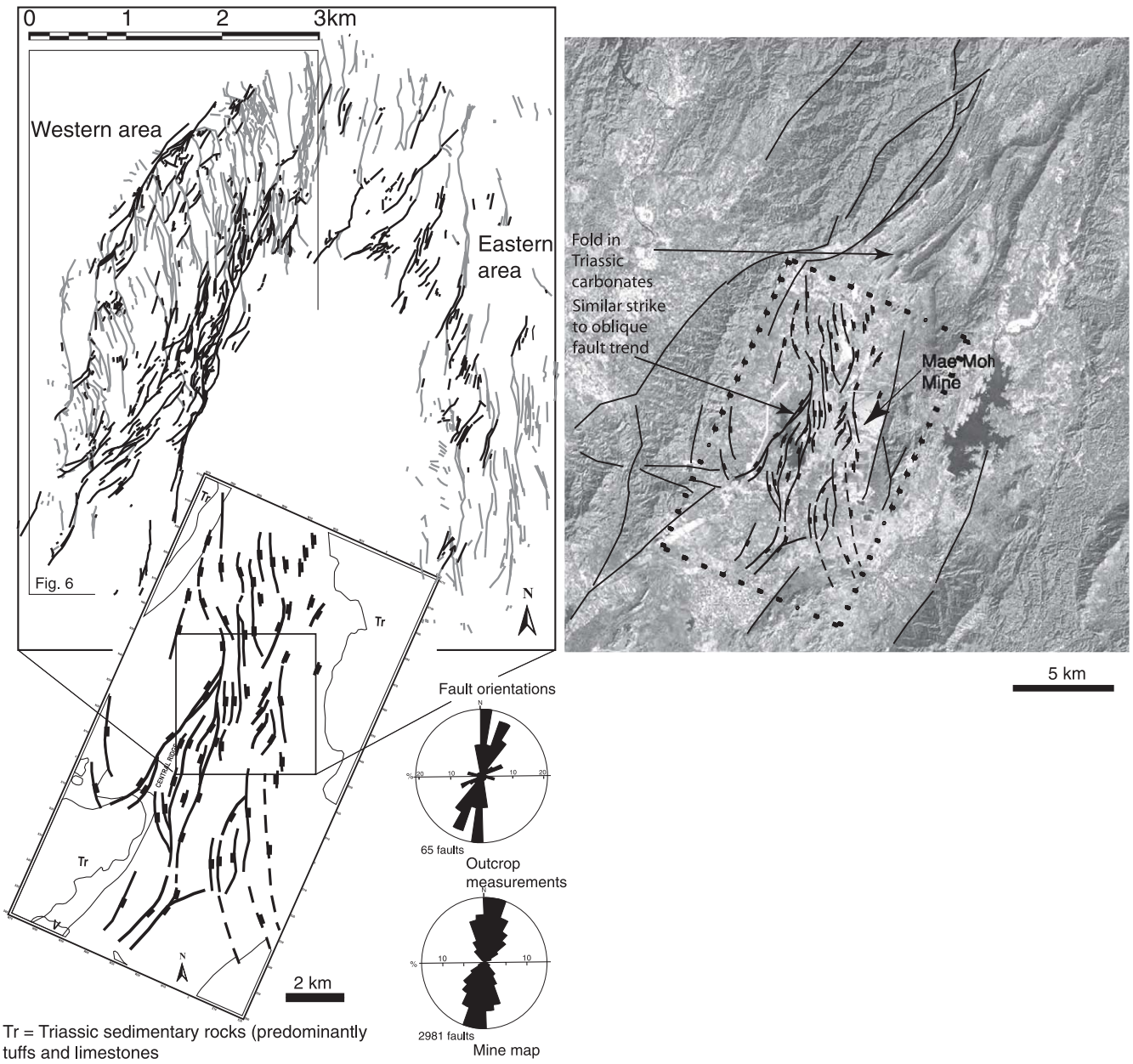

Fig. 5. Location map for Mae Moh basin and mine, with a detailed fault map of the main mining area. See Fig. 1 for location.

numerous oblique barriers to propagation (faults of opposite dip, and/or oblique strike). It was the oblique NE–SW faults that managed to propagate and link early, and inhibit the development of the rift orthogonal faults.

5.2. The Uttardit Fault: a large, discrete oblique fabric

The Uttardit Fault zone strikes ENE–WSW and bounds the northern part of the Oligocene–Pliocene Phitsanulok rift basin It follows an old Indosinian Orogeny structural trend, and lies close to the Nan–Uttardit suture (Fig. 9). The Uttardit Fault zone is a very important feature for understanding the origin of rift basins onshore because it is the only major oblique fault zone associated with a syn-kinematic sedimentary basin that is extensively crossed by seismic reflection data. The fault zone was interpreted by Polachan et al. (1991) as a major Tertiary strike-slip fault zone involved in escape tectonics. The implication of this model is that the fault zone should display predominantly sub-horizontal displacement, and act as a conjugate fault to the Mae Ping Fault zone, with the fault extending south to meet the Mae Ping Fault zone (Knox and Wakefield, 1983; Flint et al., 1988). However, mapping of 2D seismic reflection data over the fault zone indicates it is an oblique

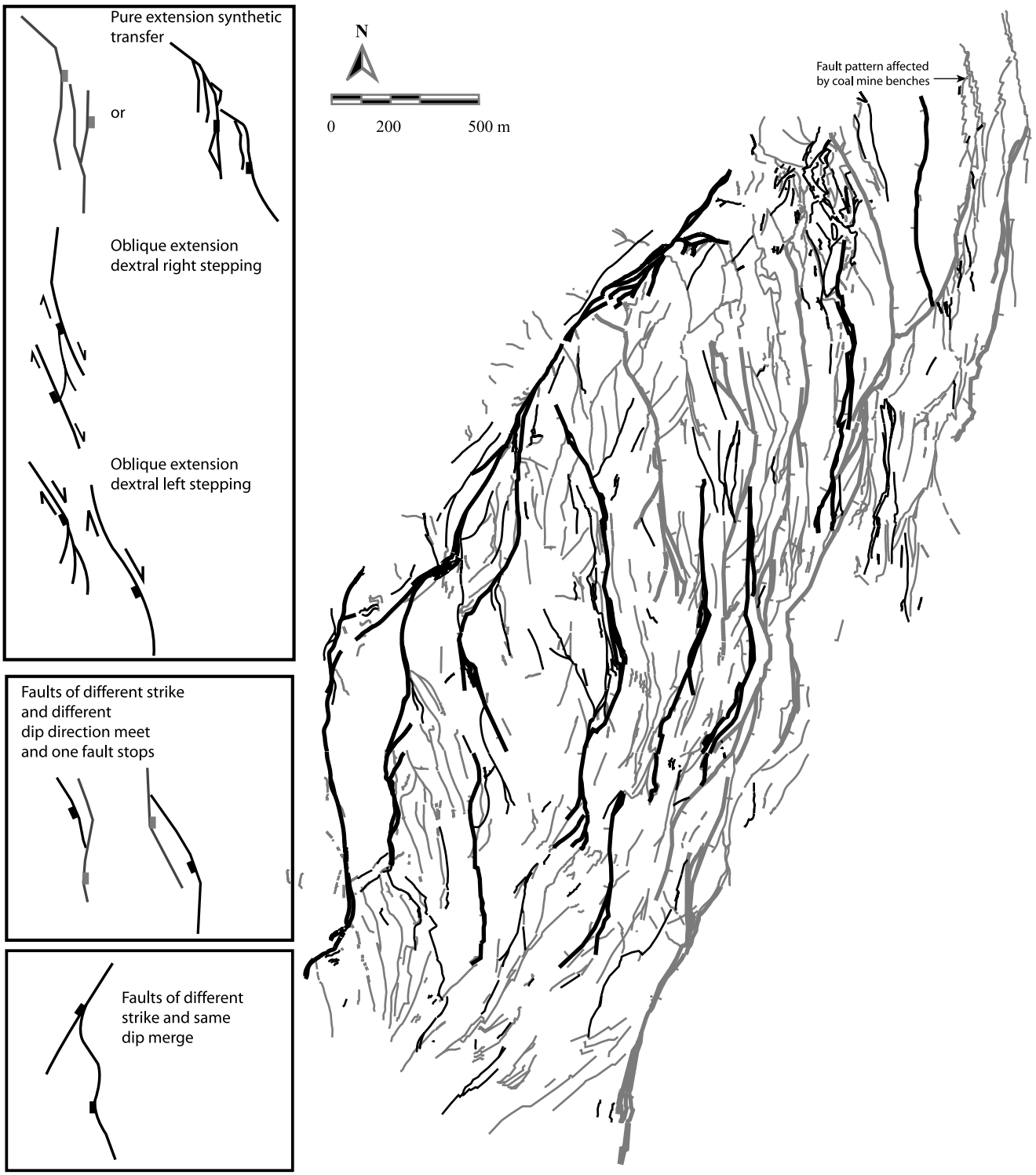

Fig. 6. Detailed fault map of the western area of the Mae Moh mine. See Fig. 5 for location.

extensional fault that follows Indosinian fabrics in basement, the evidence is described below (also see Bal et al. (1992)).

The Uttardit fault dips quite steeply to the NNW (60–75°), strikes ENE–WSW, and has one pronounced NE–SW oriented segment. The basin has a simple half graben geometry and is up to 4 km thick. The Late Oligocene–Miocene depocentre thick is located on the NE–SW-trending fault segment, which is an important indicator of oblique sinistral extension showing the NE–SW trend, which acted as a releasing bend (Fig. 10).

The major depocentre to the Phitsanulok basin to the south is focussed on the N–S striking, east-dipping Western

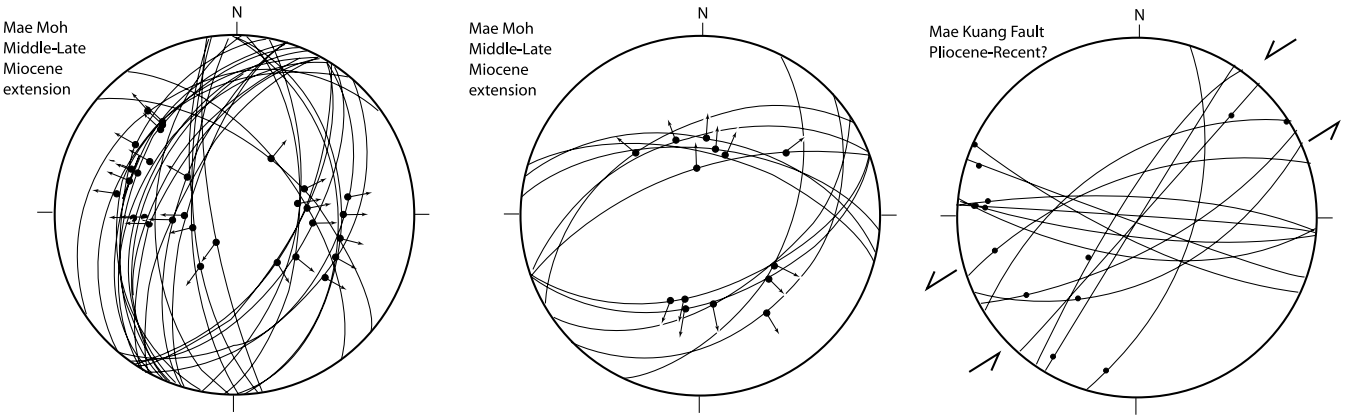

Fig. 7. Stereonets of fault orientation and slip directions for normal faults in the Mae Moh mine and strike-slip faults in the Mae Kuang fault (data from Rhodes et al. (2002)). The data illustrate predominantly E–W to NW–SE extension in the Mae Moh mine. However, slip sense tends to be sub-perpendicular to fault orientation, giving a radial extension pattern; this may be due to rotation of the stress field through time, or perhaps more likely contemporaneous slip under conditions of very low ratios between the magnitude of the maximum and minimum horizontal principal stresses (Fig. 4a). The extensional slip sense on NE–SW oriented faults from the Mae Moh mine and strike-slip sense on NE–SW striking faults from the Mae Kuang fault illustrates that variable stress conditions either spatially or temporally have affected the region and fault orientation alone cannot be used to predict slip sense (as suggested in earlier models for the region such as Polachan et al. (1991)).

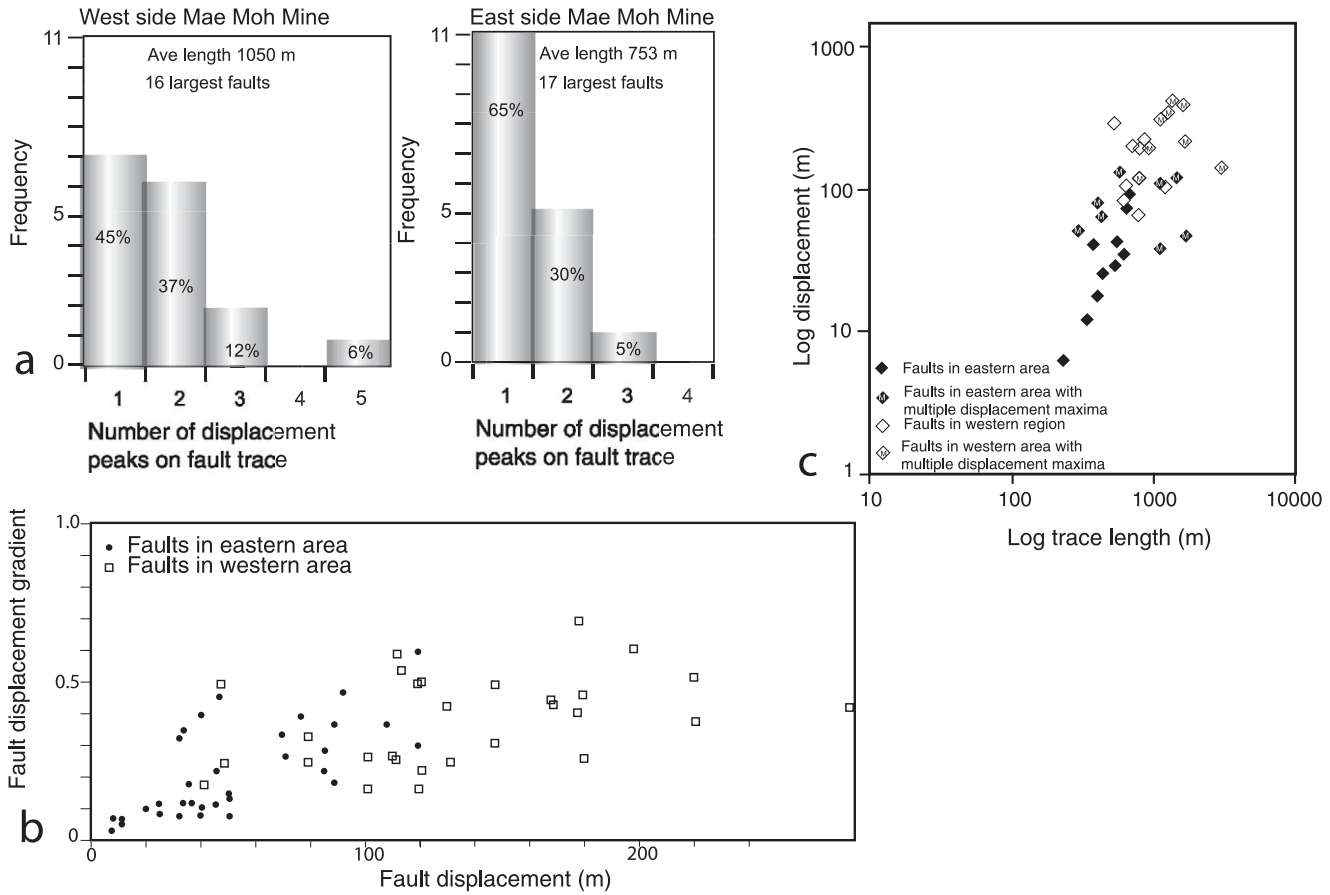

Fig. 8. Graphs illustrating some of the variation in fault population displacement and linkage characteristics between the western and eastern areas of Mae Moh mine.

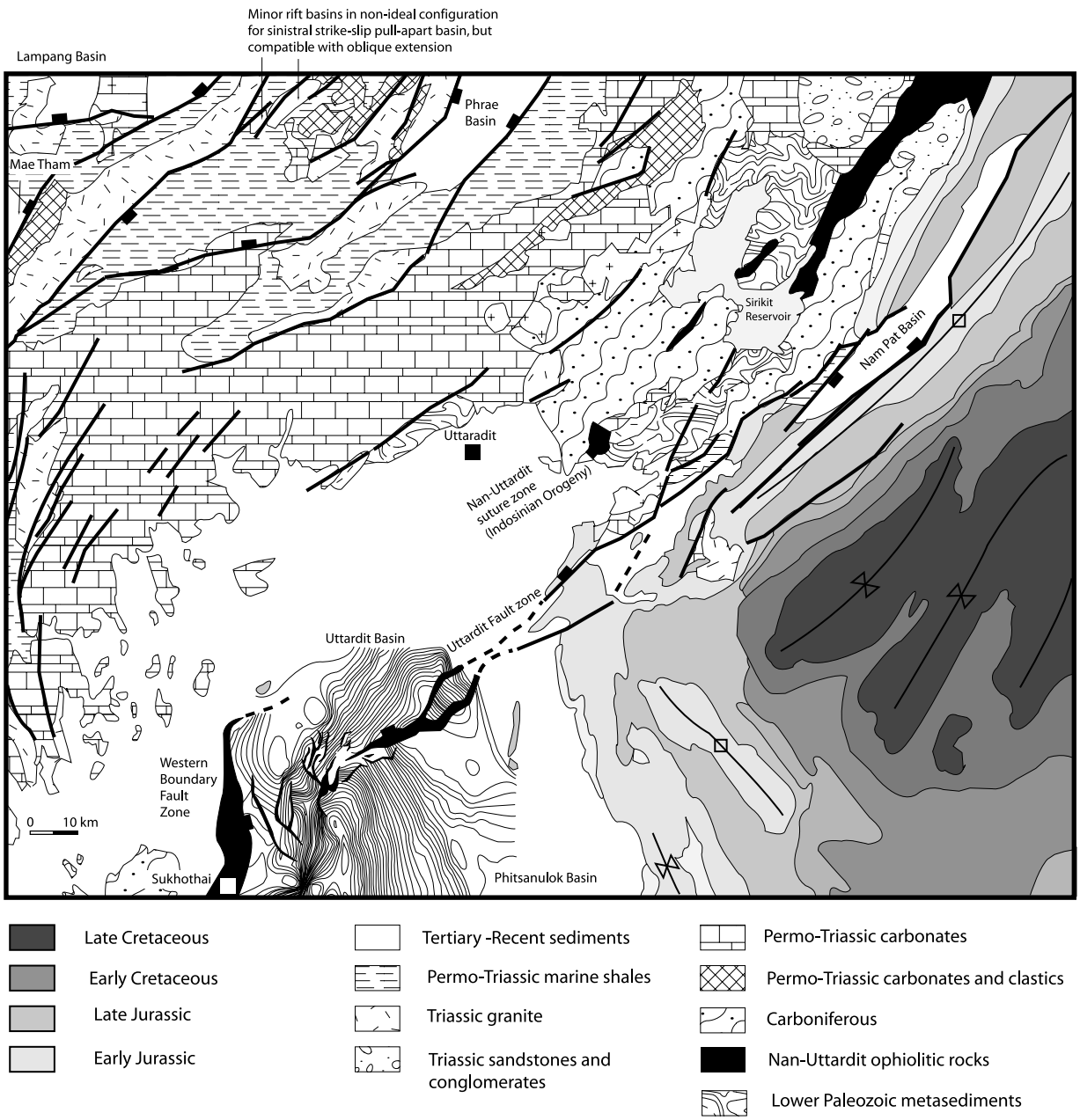

Fig. 9. Geological map of the northern Phitsanulok basin and surrounding area showing the strong ENE–WSW to NE–SW alignment of structural trends in basement, including the Nan–Uttardit suture (an Indosinian suture zone) and later Mesozoic–Paleogene folds (both NE–SW and NNW–SSE trends). These trends have later influenced the orientation of Tertiary extensional faults, giving rise to a dominant NE–SW direction, and less frequent N–S trends (pure extension trends). Data compiled from Fenton et al. (1997), Department of Mineral Resources (2001) and interpretation of 2D seismic reflection data. See Fig. 1 for location.

Boundary fault. It has a maximum 7 km of syn-rift section in its hanging wall with the depocentre located on the central N–S striking segment of the fault (Bal et al., 1992). Passing northwards, the Western Boundary fault curves to a ENE–WSW orientation directly along strike from the Uttardit fault. Hence instead of a through-going strike-slip fault trend at which the Western Boundary fault should either terminate or be offset, there is actually a co-linear transfer zone between SSE and NNE dipping oblique trending extensional fault segments. Associated with these oblique trends are basins of opposite thickening direction. The faults gradually lose displacement passing towards each other, and overlap back-to-back in a transfer zone. On the southern side of the transfer zone en échelon, normal faults are present (Fig. 10).

Under oblique sinistral extension the southern side of the western Uttardit fault tip is the extensional side of the fault tip. The northern (hanging wall) side of the western tip contains an inversion anticline that developed contemporaneously with Miocene deposition in the Uttardit basin

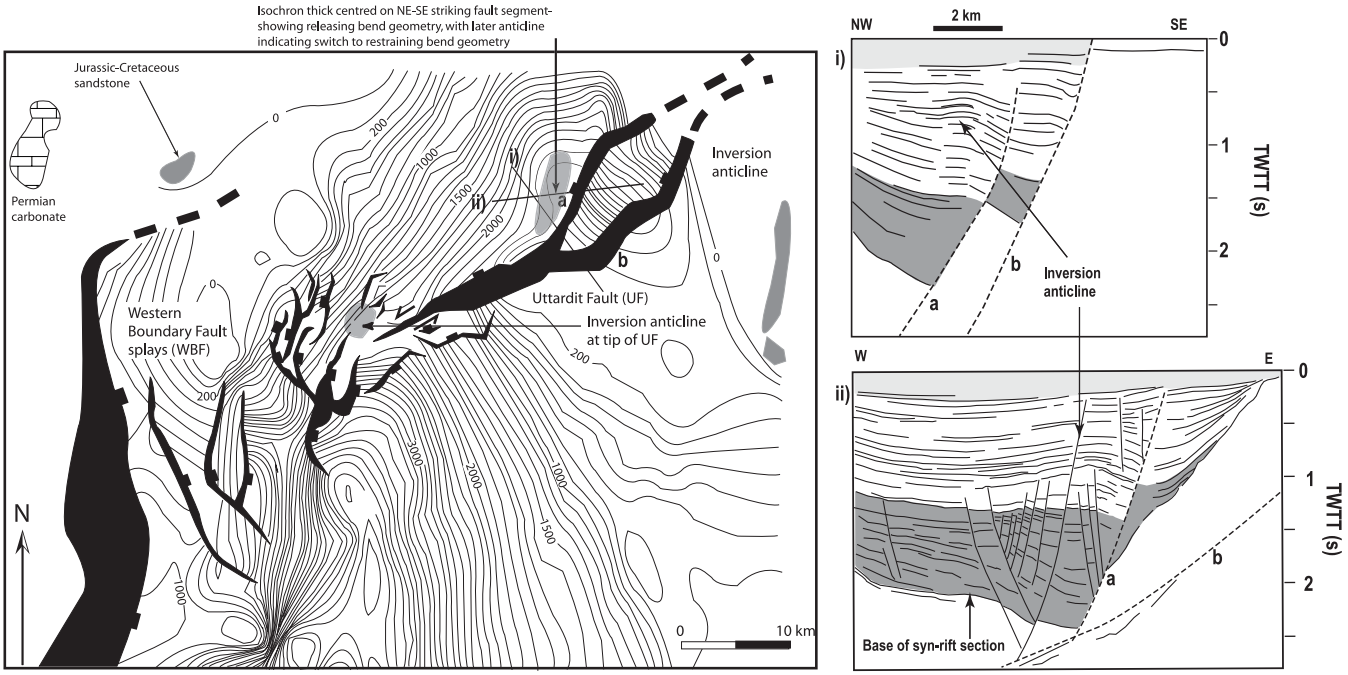

Fig. 10. Detailed time-structure map of the Northern Phitsanulok basin and cross-sections based on interpretation of 2D seismic reflection data. The data illustrates that the Uttardit fault zone is an oblique extensional fault, which dies out towards the SE and displacement is transferred from the NNW dipping Uttardit fault to the SSE dipping Western Boundary fault. The geometries are predominantly extensional, not strike-slip. However oblique extension has caused inversion at the compressional tip of the Uttardit fault, and enhanced subsidence at the NE–SW striking releasing bend orientation of the fault zone. See Fig. 9 for location.

(Fig. 10). It is the only inversion feature of this age in the area (Fig. 10). Hence this local inversion feature is interpreted as being caused by compression at the tip of the Uttardit fault, due to oblique extension with a sinistral slip component.

Evidence for fluctuating stress regimes is seen by later folding of the Uttardit basin depocentre adjacent to the NE–SW fault segment of the boundary fault (Fig. 10). To produce the folding requires a stress regime that caused inversion of the boundary fault by either dextral motion (with the NE–SW segment acting as a restraining bend) or compression. These requirements suggest Shmax trending between WNW–ESE and NNW–SSE orientations. The southernmost splay of the Uttardit fault cuts very high in the section near the land surface (Fig. 10) and displays late extensional displacement. The evolution of the fault zone is not consistent with a simple strike-slip story as suggested by Polachan et al. (1991), instead it is more consistent with a stress regime that for most of the time favoured E–W extension, but changed episodically to cause inversion.

6. Stacked layers of inheritance—the Pattani Basin

The Pattani Basin lies in the Gulf of Thailand (Fig. 1) and is the most productive basin for hydrocarbons in Thailand (e.g. Bustin and Chonchawalit, 1995; Jardine, 1997). Morley et al. (2001) and Morley (2001) provide regional reviews of the tectonic setting of the Tertiary rift basins in Thailand. The Pattani Basin is attributed an Oligocene–Middle Miocene syn-rift section and a Middle Miocene–Recent sag basin sequence by Jardine (1997) and Lockhart et al. (1997) (Fig. 11). An Eocene age to the lowest syn-rift units is a distinct possibility but there are no well penetrations of the deepest units. More recent 3D seismic data show the structural development is more complicated. A well developed Eocene (?)–Oligocene syn-rift sequence is present and eroded syn-rift topographic features such as tilted fault blocks and horsts are capped with angular unconformity by late Oligocene reflections. The largest syn-rift faults have displacements up to a few kilometres. The late Oligocene appears to mark the onset of thermal subsidence. However, extension on numerous syn-rift faults continued into the Lower Miocene, the largest associated faults display offsets of hundreds of metres. Hence the early post-rift thermal subsidence overlapped with extensional activity. Subsequently, from the Middle Miocene onwards a set of distinctive, relatively small displacement (tens to a few hundred metres displacement), conjugate normal fault

Fig. 11. Regional fault map of the Pattani Basin based on 2D and 3D seismic reflection data, illustrating fault patterns in the Late Oligocene–Early Miocene syn-rift section and Middle Miocene–Recent post-rift section, compiled from unpublished maps made by Unocal (see Fig. 1 for location). Rose diagrams show fault orientations for the post-rift section for areas discussed in this paper.

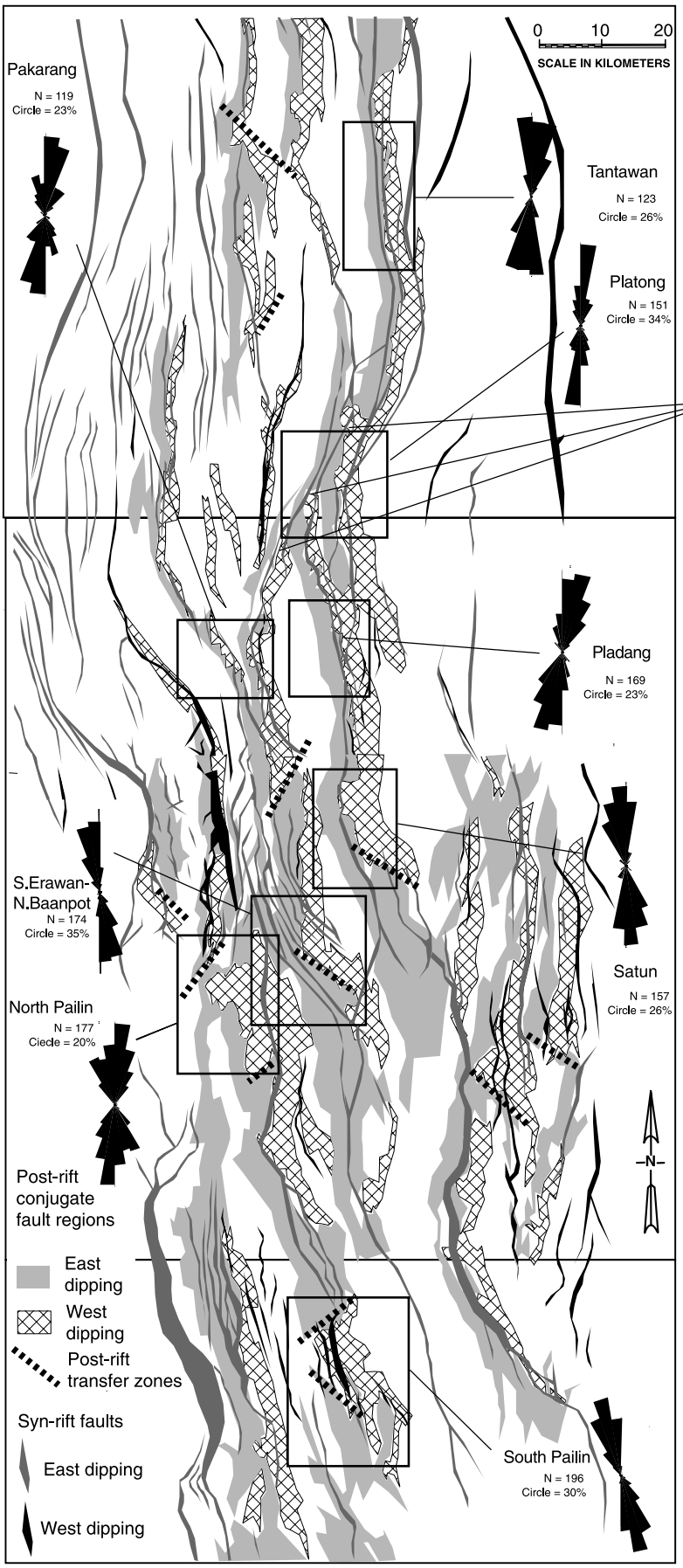
0 10 20
SCALE IN KILOMETERS
Pakarang
N = 119
Circle = 23%
Tantawan
N = 123
Circle = 26%
Platong
N = 151
Circle = 34%
Pladang
N = 169
Circle = 23%
S.Erawan-
N.Baanpot
N = 174
Circle = 35%
North Pailin
N = 177
Ciecle = 20%
Satun
N = 157
Circle = 26%
South Pailin
N = 196
Circle = 30%
–N–
Post-rift
conjugate
fault regions
East
dipping
West
dipping
Post-rift
transfer zones
Syn-rift faults
East dipping
West dipping
Northern Province
3 pairs of
convergent faults
N-S trends
Termination of
3 convergent fault
pairs at oblique
sequence 1
fault zone
Central Province
Zone of oblique
trends short
zones of
convergent faults
NW and NE trends
Very broad zone
of conjugate faults
(up to 7 pairs of
convergent faults)
Mostly N-S
orientation. Short
NW to NE oblique
trends
Southern Province
2-3 pairs of
convergent
faults
NNW orientation

systems affect the post-rift section (Fig. 11). Structural traps for hydrocarbons in the Pattani Basin are unusual for rift-sag sequences: the large fields are associated with broad, low-relief anticlinal structures formed within the grabens of converging conjugate normal fault systems in the post-rift section (Fig. 11).

In map view the post-rift (PR) conjugate fault form linear zones where all faults dip in the same direction, typically to either the west or the east. Passing along strike these zones undergo abrupt reversals in fault dip (Fig. 11) along narrow, oblique trending transfer zones that are locally known as graben shifts. The origin of these graben shifts is not clear, although at different scales they appear to be a typical characteristic of conjugate normal faults in any structural setting. However, a recent study of the Funan Field (Kornsawan and Morley, 2002) using 3D seismic data demonstrated that transfer zones within one conjugate fault set were inherited from the underlying distribution of faults in the syn-rift section. In turn faults in the syn-rift section inherited fabrics from the pre-rift section, in particular NW–SE and NE–SW trends (Kornsawan and Morley, 2002).

Regional fault maps of the Oligocene–Early Miocene syn-rift (SR) and Middle Miocene–Recent post-rift (PR) sequences made by Unocal from 2D and 3D seismic data are discussed below. These maps illustrate how syn-rift structures affected post-rift conjugate faults on a regional scale. Two levels of influence are discussed: (1) regional comparisons between the major syn-rift faults and the geometry of east- and west-dipping post-rift dip provinces, and (2) detailed examination of interactions between individual faults in the post-rift and syn-rift sections.

7. Regional maps of the Pattani Basin

7.1. Regional syn-rift fault pattern

The regional fault pattern for Sequence 1 (early syn-rift) in the Pattani Basin (Fig. 11) shows that in the northern part of the basin east-dipping faults dominate, the main depocentre lies on the eastern side of the basin. Passing south towards the central area is a NE–SW oblique trend, characterised by a broad area composed of three main depocentres. Some NW–SE trends are present. To the south NW–SE trends become common, and in the southern-most part of the area the main depocentre lies on the western side of the basin. Transfer zones between the major faults are typically overlapping synthetic and mostly soft-linked, hence relay ramps are common features. Most of the major bounding faults are east-dipping. Major west-dipping faults are uncommon, the most important west-dipping fault occurs in the western central area. The major faults are commonly 40–80 km long and rarely exceed maximum throws of 3 km. Multiple depocentres on some faults suggest linkage of originally separate faults (Kornsawan and Morley, 2002; Fig. 12). Faults commonly turn into NW–SE and NE–SW oriented segments, or terminate along these lines, suggesting the presence of basement fabric trends underlying the rift (Figs. 11 and 12).

Fig. 12 shows one detailed example from the southern Pattani Basin where strong NW–SE and NNW–SSE trends affect the basin. The absence of strike-slip offset of large faults and oblique alignment of secondary faults and jogs in major faults along oblique trends indicates the influence of passive basement fabrics. A dominant NW–SE alignment of sedimentary facies belts during the early stages of rifting in the Oligocene changes to a N–S direction in the Miocene N–S (Lockhart et al., 1997). This change may be due to a rotation of the extensional stress field, but equally likely could be that as the rift evolves the optimally oriented faults became dominant and the oblique faults became less active, as discussed in the mechanics of oblique extension section (Fig. 2b).

7.2. Regional post-rift fault pattern

The PR faults are much shorter (typically 2–20 km long), have smaller displacement (rarely exceeding 300 m), and are more numerous than the SR faults. The longer PR faults show evidence of multiple linkage of shorter (2–4 km long) faults, both from linkage geometries (splays, bends, horses) and multiple depocentres. Mapping of hundreds of PR faults from seismic reflection data shows they occur in discrete east- and west-dipping packages that comprise convergent conjugate fault sets.

Important transfer zones (graben shift) between the west- and east-dipping PR fault sets are marked by abrupt incursions of one dip set into the area that along-strike is occupied by the other dip set (Fig. 11). The boundaries between the two fault dip domains in the transfer zones trend NE–SW, NW–SE or E–W. The transfer zones can take the form of salients and re-entrants between two parallel bands of fault dip domains, or at the end of a fault dip domain.

The total length of east-dipping faults in the syn-rift section is 2.3 times that of west-dipping faults, suggesting east-dipping basement fabrics have influenced syn-rift fault dip. The preponderance of the east-dipping orientation is transferred to the post-rift section: the area occupied by east-dipping fault swarms is about 50% greater that that of the west-dipping faults (also see Fig. 11). As discussed in Anderson (1951), once a fault affects a volume of rock, the differential stress drops in the volume around the fault. The stress drop tends to inhibit conjugate shear development, but will favour spaced development of a packet of synthetic faults. Consequently the relatively early development of a single post-rift fault whose dip is related to a syn-rift fault will influence an array of synthetic faults that are not necessarily linked with basement faults.

The conjugate fault systems in the northern Pattani Basin comprise 3–4 systems of east- and west-dipping convergent conjugate fault set pairs. The central province is composed

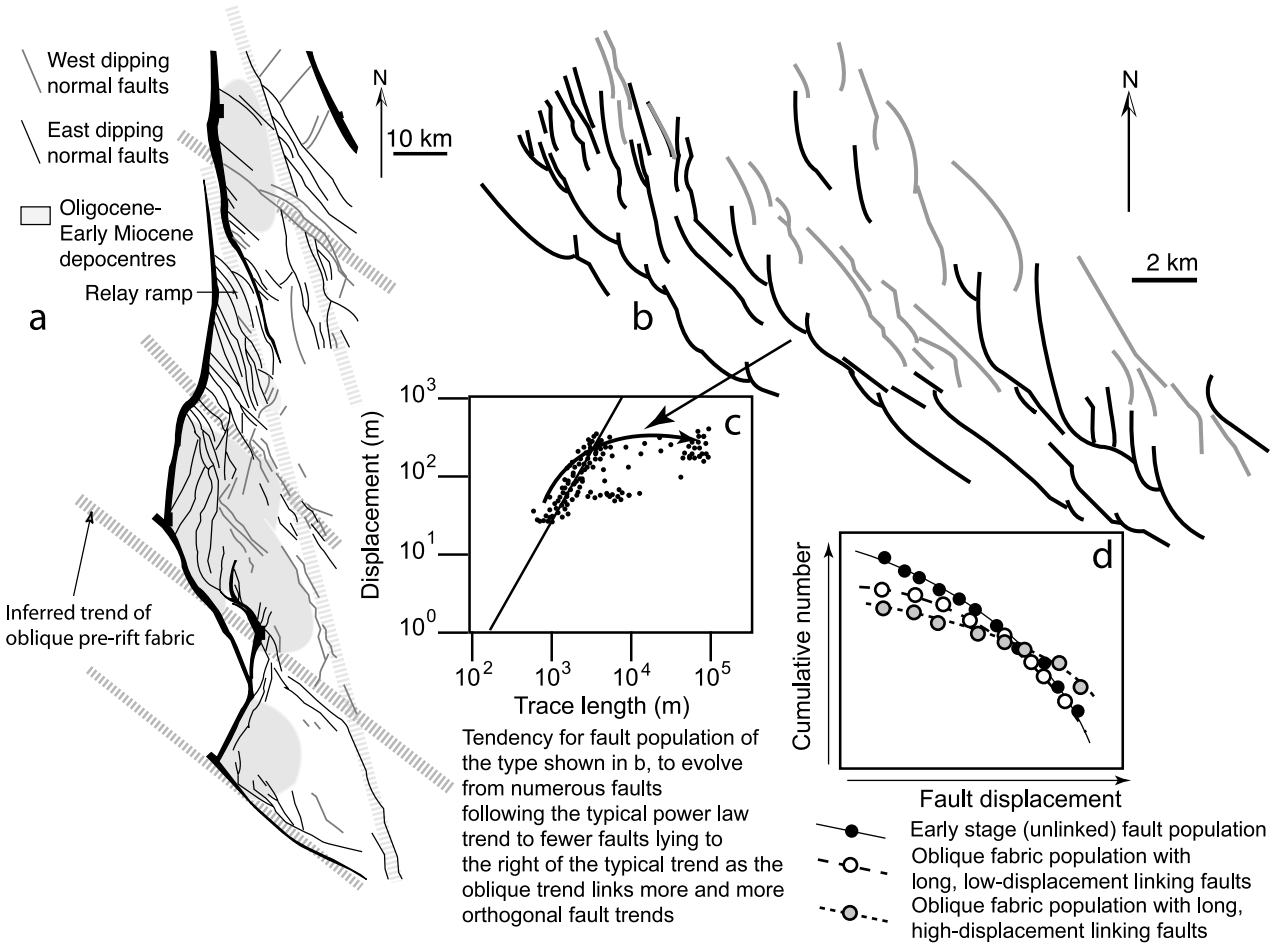

Fig. 12. Structure maps of two areas in the southern Pattani basin–Northern Malay basin area. (a) Syn-rift structure map illustrating strong NW–SE trends with affect some of the syn-rift faults (redrawn from Lockhart et al. (1997)). (b) Post-rift fault trends from the Northern Malay basin area (redrawn from Morley (2001)), illustrating inheritance of NW–SE fabrics from the syn-rift section. The importance of the oblique orientation has increased from that shown in (a), and shows how variations in the importance of N–S and NW–SE elements produces significantly different fault patterns. See Fig. 1 for location.

of 5–8 conjugate fault sets, whereas passing to the south only 2–3 conjugate fault trends are present (Fig. 11). The changing number and location of the post-rift conjugate fault zones closely follows the changing syn-rift patterns. The syn-rift faults occupy a few discrete trends in the north and south, whilst in the central area syn-rift faults form a broad distributed network. Hence the syn-rift section appears to apply important seed faults that determine the number, location and orientation of the conjugate fault sets. However, the conjugate faults are not entirely influenced by the syn-rift structure, in places conjugate faults form where no syn-rift faults are present, or they strike at different orientations to the underlying syn-rift faults.

8. Examples of detailed fault interactions in the Pattani Basin

8.1. Conjugate fault interactions

The interaction of conjugate fault sets at a regional scale described above showed that abrupt changes in post-rift fault dip province orientation at transfer zones are linked with changes in the syn-rift fault pattern. However, to understand how the syn-rift and post-rift fault packages are related, it is necessary to identify the variety of ways in which individual faults in the post- and syn-rift sections have interacted; to accomplish this, seven areas (Funan, Tantawan, Pladang, Parakang, South Palin, Platong and Satun Fields) were investigated from 3D seismic data, six areas are described below whilst the Funan field is described in Kornsawan and Morley (2002).

Conjugate faults in cross-section can intersect in a variety of ways (e.g. Horsfield, 1980; Nicol et al., 1995; Watterson et al., 1998) but basically fall into two groups: either (1) the faults display cross-cutting relationships or (2) locally one dip set is dominant and the other dip set stops above or at the dominant fault plane. In the Pattani Basin most conjugate faults fall into type 2, with type 1 only rarely occurring. Most conjugate faults die out downwards within the Tertiary section. Some faults, however, either vertically link with syn-rift faults and thus pass into pre-rift basement,

or pass into pre-rift basement independently of syn-rift faults and thus inherit pre-existing fabric orientations. The vertically linked faults with their inherited strikes and dips exert an influence on the development of fault patterns in general, and specifically at transfer zones.

Conjugate fault patterns in experiments and nature commonly display along-strike fluctuations in the dominant polarity of opposite-dipping fault systems (Nicol et al., 1995; Kornsawan and Morley, 2002; McClay et al., 2002). In a propagating system of faults of initial random dip directions in rock with isotropic strength, transfer zones between different fault dip provinces are bound to evolve. However, the presence of pre-existing fabrics may accentuate the characteristics of how changes in polarity are accomplished and localise where polarity changes occur. For example Keep and McClay (1997) commented on an experimental model that "persistent first-phase faults caused boundary fault segmentation and salients and embayments along the boundary faults during the second deformation phase". The geometry of such interactions is described below.

8.2. Pladang Parakang and Tantawan Fields

The Pladang and Tantawan Fields illustrate fault patterns in areas outside of the syn-rift transfer zones. Fig. 13 shows that syn-rift faults have major NNW–SSE to N–S and minor NNE–SSW fault trends. In contrast the post-rift faults displays major NNE–SSW to NE–SW trends and minor NNW–SSE trends. The conjugate fault package is bounded by long NNW–SSE-trending faults (e.g. E-400P), whereas internally short NE–SW trends predominate. For the Pladang Field the east-dipping E-400P fault is linked with the syn-rift fault, hence its orientation reflects inheritance of a pre-existing fabric. Harder to explain are the NNW–SSE-trending W-314N and W-362 faults, for which there is no underlying west-dipping syn-rift fault. These faults presumably formed as antithetic faults to E-400P and were directly influenced by the development of that fault, unlike the internal fault sets. The NNE–SSW faults of opposite dip show slightly overlapping configurations, and produce conjugate convergent overlapping transfer zones (Fig. 13). The Tantawan Field time structure map (Fig. 13) shows that there is little difference in displacement amount between the short and long post-rift faults, with depocentres actually tending to be better developed along the short NE–SW faults, than the long N–S faults. Somewhat similar interactions between two stages of faulting (one orthogonal, one oblique) have been produced by experimental modelling of multi-stage rifts (Bonini et al., 1997; Keep and McClay, 1997).

The Parakang Field overlies a region in the syn-rift section that passes from N–S striking syn-rift faults in the south to NNW–SSE and NE–SW trends passing north (Fig. 13). The syn-rift faults display overlapping synthetic transfer zones. The post-rift section exhibits a similar geometry to that described for the Pladang and Tantawan Fields: the outer faults to the conjugate set follow the strikes of the syn-rift faults, the internal post-rift faults tend to strike NE–SW, but curve to join the long outer faults. The syn-rift en-échelon fault sets form relay ramps in synthetic transfer zones with the fault tips aligned along a NW–SE trend. The post-rift faults form a NW–SE-trending left stepping zone above the syn-rift synthetic transfer zone (Fig. 13).

8.3. South Palin Field

The South Palin Field displays a map-view salient in the west-dipping, post-rift faults (Fig. 14) similar to that described for the Funan Field by Kornsawan and Morley (2002). The salient overlies a narrow zone where west-dipping, syn-rift faults lie along-strike from east-dipping faults (Fig. 14). The northern boundary of the salient arises from the dip direction of a N–S striking basement thrust fault. The pre-rift section displays strong reflections with similar geometries on successive dip lines, where a sedimentary section appears to be folded and eroded below the unconformity with the syn-rift section. From regional considerations it is likely that the reflective pre-rift section is Permo-Triassic carbonates folded during the Indosinian orogeny, or Mesozoic sedimentary rocks folded during Late Cretaceous–Early Tertiary transpression. An east-dipping thrust cuts through the centre of the high and exhibits a footwall ramp, hanging wall flat geometry. The fold axial planes trend approximately N–S. The low-angled listric thrust fault is similar in style to those imaged in the Khorat Plateau to the northeast (e.g. Cullen et al., 1997). A horst block is present between the overlapping, opposite dipping, syn-rift fault sets. In the north, east-dipping fault sets dominate, and appear to sole into the basement thrust plane, giving rise to relatively low-angle normal faults. Passing south, west-dipping faults, which cross-cut basement reflections, become important, the basement thrust geometry becomes less distinct and is no longer followed by later normal faults.

Fig. 13. Fault maps derived from 3D seismic data of superimposed syn-rift faults and post-rift faults illustrating which post-rift trends are controlled by syn-rift faults and which trends are independent. Pladang, Tantawan and Parakang Fields are shown; see Fig. 11 for location. Tantawan Field area of the Northern Pattani Basin, Gulf of Thailand (redrawn from Rigo de Rhigi et al. (2002)). Time-structure map on a Miocene horizon based on 3D seismic interpretation, depth of contours not specified but contour interval is every 100 milliseconds two way travel time, with the darker fills corresponding with greater travel times (i.e. deeper section). Black fault faults dip towards the east to southeast, white faults dip towards the west to northwest.

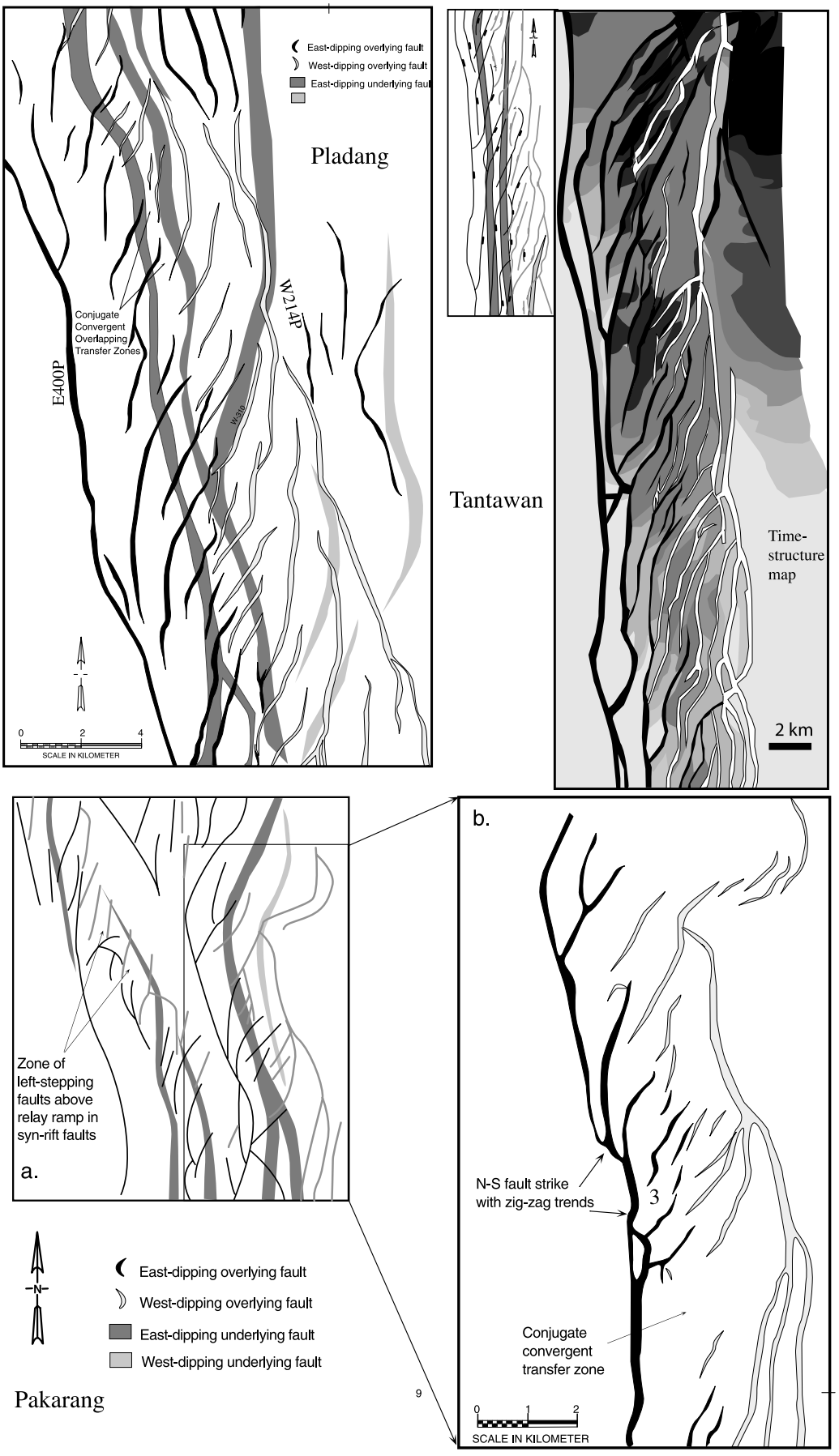
East-dipping overlying fault
West-dipping overlying fault
East-dipping underlying fault
Pladang
W214P
E400P
Conjugate
Convergent
Overlapping
Transfer Zones
0 2 4
SCALE IN KILOMETER
Tantawan
Time-
structure
map
2 km
Zone of
left-stepping
faults above
relay ramp in
syn-rift faults
a.
b.
N-S fault strike
with zig-zag trends
3
Conjugate
convergent
transfer zone
0 1 2
SCALE IN KILOMETER
East-dipping overlying fault
West-dipping overlying fault
East-dipping underlying fault
West-dipping underlying fault
Pakarang
9

8.4. Satun Field

In Satun field one east-dipping syn-rift fault is present, with NNW–SSE, N–S and NNE–SSW striking segments (Fig. 15). In the post-rift section the west-dipping fault sets step westwards in two distinct zones, to form an asymmetric salient. The salient coincides with a broad U-shape in the syn-rift fault; this curvature is more pronounced in the east-dipping post-rift fault E-350P, which is a composite of several faults, it links down-dip with syn-rift fault E-400S. The subtle change in syn-rift fault geometry appears to have exerted a more pronounced effect on the post-rift faults.

8.5. Platong Field

Platong Field lies at a change from N–S to NE–SW syn-rift fault orientations. The post-rift fault pattern shows predominantly N–S to NNW–SSE trends, and one long NNE–SSW-trending fault (E-1), which is linked at depth with the syn-rift fault E (1) (Fig. 15). In area B a salient of west-dipping faults extends westwards about 2 km into the east-dipping fault province. The northern margin of the salient coincides with the change from a N–S to NE–SW strike in the syn-rift faults. Most of the post-rift faults do not follow the NE–SW syn-rift trend, one exception being fault E-1P. This avoidance of the NE–SW pre-existing faults and predominance of N–S to NNW–SSE striking post-rift faults, suggests that at least locally the post-rift extension direction was E–W to ENE–WSW.

9. Fault linkage patterns associated with oblique fabrics

One pronounced feature of some Tertiary rift basins in Thailand is the presence of long, relatively small-displacement faults formed by the linkage of numerous relatively small faults (Fig. 16). This characteristic is seen in parts of the Pattani Basin (Fig. 13, faults E-400P, W-214P, E-29P, W-840P), and is even more strongly developed in the northern Malay basin (Fig. 12). Relatively small displacement faults striking N–S curve into a NW–SE strike on their southern tips, which serves to link a whole series of N–S faults (Fig. 16a), in parts of the basin 10–20 linked fault segments are present.

Onshore and in the Gulf of Thailand, commonly the long fault trend is N–S (following N–S striking syn-rift faults) whereas the short fault trend is NNE–SSW to NE–SW, and is independent of syn-rift fault trends (Figs. 13 and 16b). Such geometries imply that the minimum horizontal principal stress was oriented WNW–ESE to NW–SE (Fig. 16b). This marks a departure from the inferred regional E–W extension direction. Variations in the orientations of oblique structures suggest that even if the regional extension direction is E–W, locally the principal stresses may differ. For example Yale et al. (1994) described examples from the North Sea where local deflection of stress directions were due to the effects of basement structure in regions of complex faulting. A recent unpublished modern stress study conducted for UNOCAL (R. Hillis and M. Tingay, pers. comm., 2001) showed considerable variation in orientation of the maximum horizontal principal stress directions (between NE–SW and NW–SE, but predominantly N–S). This is similar to earthquake focal mechanisms for onshore Thailand that show predominantly strike-slip solutions with NNW–SSE to NE–SW oriented maximum principal stress directions (Bott et al., 1997).

In central Thailand pre-rift oblique fabrics trend predominantly NE–SW and NW–SE (Fig. 1). The NW–SE striking, 10–30-km-wide faulted zones of the Mae Ping and Three Pagodas faults have an effect on the rift basins. The border fault of the Ayattuya half graben curves into a NW–SE trend along the strike of the Mae Ping fault and the northern limit of the Suphan Buri basin lies at the Mae Ping fault (Fig. 1). The Three Pagodas fault causes a left-stepping offset between the Kamphaeng Saen basin and the Sala Daeng (or Thon Buri) basin (O'Leary and Hill, 1989).

At a smaller scale the boundary fault to the Supan Buri Basin has a general N–S trend but splays frequently branch off the main boundary fault and strike NE–SW. The boundary fault appears to be composed of tens of these splays with NE–SW to N–S striking segments that created minor depocentres that subsequently linked (Ronge and Korakot, 2002), leaving a series of along-strike undulating highs and lows similar to the fault schematically illustrated in Fig. 16c; a similar geometry on NW–SE oblique fabrics is shown for the southern Pattani Basin in Fig. 12. The geometry is somewhat similar to that described above for the Northern Malay basin (Fig. 12), except the N–S trend is dominant instead of the NW–SE orientation.

There is an important difference between the N–S faults with NE–SW splays discussed for the post-rift Pattani Basin section (Fig. 13) and those in the Suphan Buri basin (Fig. 16b and c). In the former the N–S trend is the inherited fabric and the extension direction is NW–SE; in the latter, it is the NE–SW splays that follow the inherited fabric (during E–W extension) (Fig. 16b and c). Hence, misleading interpretations can be made if the fault pattern alone is interpreted without knowing the orientation of the pre-existing fabric.

10. Differences between oblique extension, orthogonal extension and strike-slip faults

Zig-zag, en-échelon and stepping map-view fault geometries are present in extensional, strike-slip and oblique slip fault systems. They are not unique to any one system. However, some of the variations of structural style, depocentre location and geometry provide important indicators for determining under what deformation style or

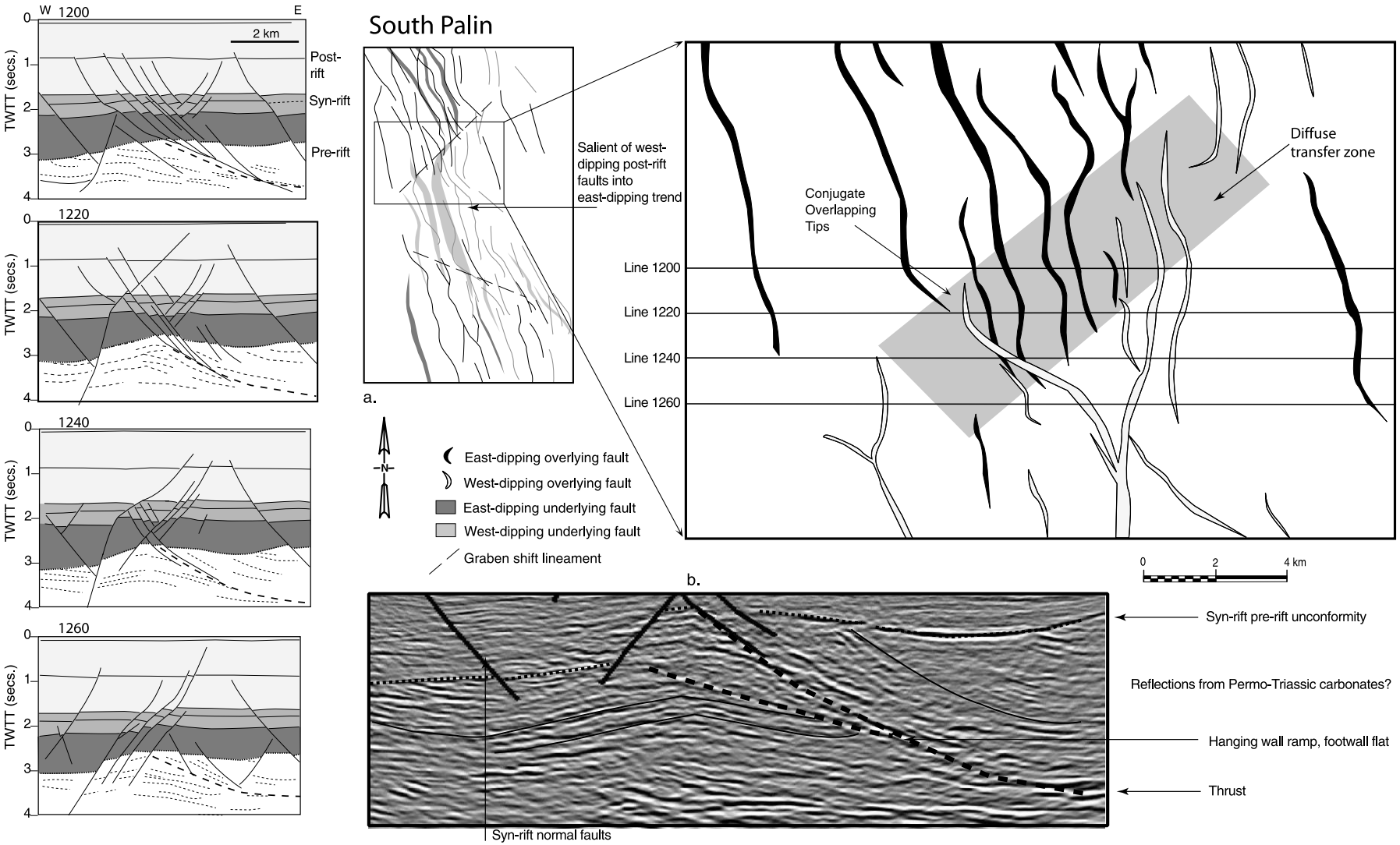

Fig. 14. Example of the influence of a non-oblique pre-existing fault influencing syn- and post-rift dip trends, South Palin Field. Lower angle east dipping fault follow a low-angle basement thrust in the northern part of the area. In the southern part of the area the thrust is not followed by the faults and west-dipping faults dominate.

Fig. 15. Fault maps derived from 3D seismic data of superimposed syn-rift faults and post-rift faults illustrating which post-rift trends are controlled by syn-rift faults and which trends are independent. Satun, Platong and South Erawan Fields are shown; see Fig. 11 for location.

styles the faults developed. These characteristics are discussed below and are summarised in Fig. 17.

Large, simple, pure extensional fault systems have the following common characteristics. (1) They tend to form overlapping arrays of faults and en échelon patterns are common. For synthetic, en échelon fault sets there is no difference in structural style between left and right-stepping fault sets. (2) Any oblique-trending fault segments (to the regional extension direction) exhibit predominantly extensional offsets. (3) Basins develop in the hanging wall of the faults and are elongated parallel to the strike of the fault. (4) Minor faults may branch off larger extensional faults with a broad range of angles, forming splays, horses and oblique-slip transfer faults. Commonly these faults are developed in response to the effects of oblique fabrics or fault linkage. (5) Striations on the fault surface are predominantly dip-slip.

Master strike-slip faults have the following characteristics (for reviews see Sylvester (1988) and Woodcock and Schubert (1994)). (1) They form narrow linear overlapping arrays of faults; en échelon patterns are common. The sense of lateral motion on the fault and stepping sense of en échelon arrays has important differences: for dextral faults right stepping geometries are extensional, and left stepping geometries are compressional, the opposite pattern applies to sinistral motion. (2) Oblique-striking fault segments provide vital clues about fault displacement sense forming either restraining or releasing bends. (3) Basins can form in a variety of locations along strike-slip faults; however, their most common location is the 'pull-apart' type setting which occurs between en-échelon faults with an extensional sense (i.e. right-stepping left lateral and left-stepping right lateral fault systems), or at releasing bends. (4) Subsidiary faults associated with major strike-slip faults are the primary wrench features (R, R′, P and Y shears). (5) Striations on the master strike-slip fault zone will be predominantly sub-horizontal. Along secondary faults and at jogs more oblique-slip and dip-slip striations may develop.

Experimental models provide some examples of the differences between how orthogonal extension and oblique fault systems evolve and indicate that high angles of oblique extension ($\alpha = 30°$) are required before the zones of deformation start to narrow significantly, and the system resembles a strike-slip zone with R- and R′-shears starting to develop. However, these models really only investigate one or two styles of oblique extension and do not represent the potential variety of fabric interactions in nature, nor do they truly mimic the way pre-existing fabrics are distributed in the crust (Morley, 1999). Fabrics are imposed at the bottom

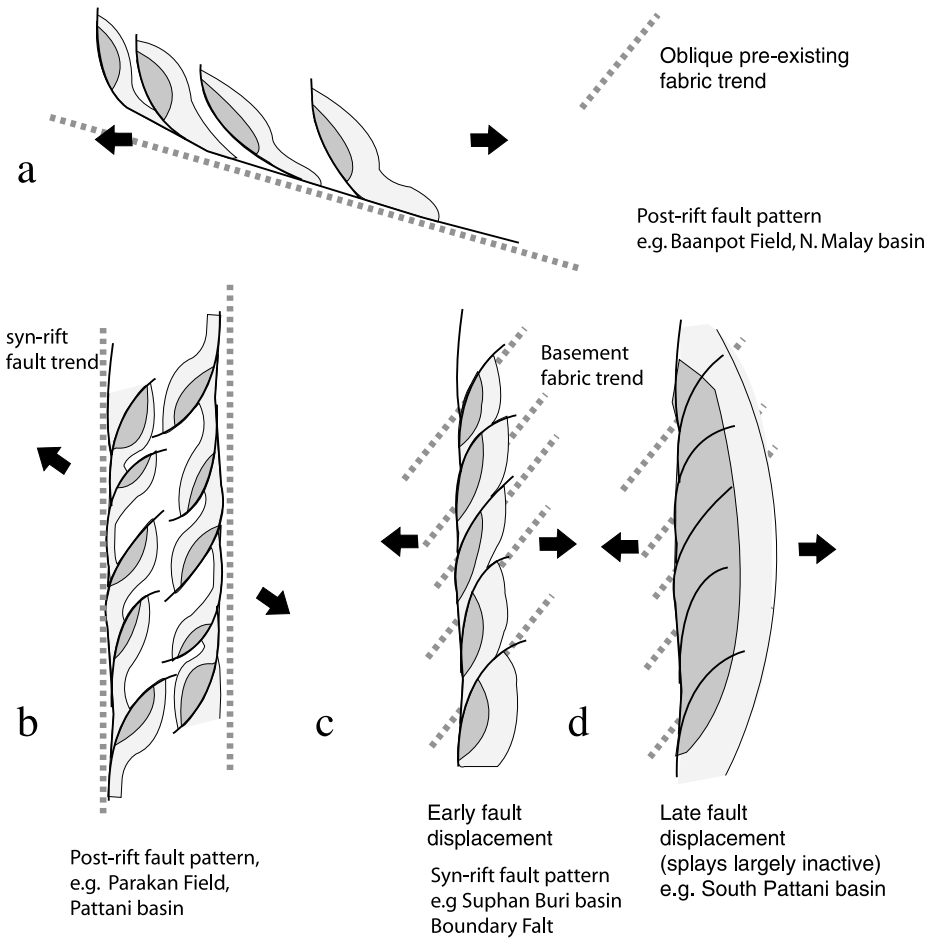

Fig. 16. Idealised illustration of the variations of map view geometries of long (tens of kilometres) major fault zones with multiple splay geometries found in the rift basins of Thailand. The influence of pre-existing fabric can lead to either splays lying sub-orthogonal to the extension direction and linking along an oblique fabric ((a) and (b)), or multiple splays following an oblique trend whilst the master fault lies sub-orthogonal to the extension direction (c). As displacement increases on the master fault the early influence of the splays on depocentre (c) location may be lost (d). Depocentres shaded grey.

of the model on the extending rubber sheet; consequently the models have a 2D fabric, whereas the crust has 3D fabrics, affecting both the strike (Figs. 9, 12 and 13), dip (Fig. 14) and transfer zone location of later extensional faults.

Zones of oblique extension occur because fabrics within the crust are sufficiently weak in oblique directions to favour failure in the oblique direction and/or at non-optimum dips compared with that produced by orthogonal extension in an isotropic material. The relative strength of the fabrics with respect to each other and the strength of intact host rock, their orientation (both strike and dip) and their spacing all serve to control the relative intensity of the oblique extensional trends relative to the orthogonal extensional trends. It is the degree to which oblique fabrics are activated that gives character to the 'oblique' deformation style (Fig. 17), not just the angle of oblique extension. However, it is the latter that is emphasised in physical models (e.g. Withjack and Jamison, 1986; Clifton et al., 2000). Even Fig. 16 is simplistic and only considers one orientation of oblique fabric. Commonly in rifts there are multiple orientations.

Oblique-slip faults can exhibit predominantly dip-slip or strike-slip motion depending upon the relative magnitude of the intermediate stress to the other principal stresses (e.g. Bott, 1959) and the angle of oblique extension. Applying simple trigonometry to calculate the striation dips on oblique faults indicates that even highly oblique faults such as the Uttardit fault (Fig. 9) will tend to display predominantly dip-slip motions (Morley, 1995). Just considering fault orientation with respect to displacement direction, the strike-slip component of displacement on even highly oblique faults (α up to 30°) will tend to only be 30% or less of the dip-slip displacement. While this simple approach may commonly apply to oblique slip zones there is also the potential for strain partitioning to cause certain faults to display predominantly strike-slip motions (e.g. Schlische et al., 2002). Larger displacements and thinner cover sequences are thought to favour strain partitioning over distributed deformation (Schlische et al., 2002).

The characteristics of oblique slip faults are as follows (Fig. 18). (1) They will form en échelon overlapping fault patterns similar to extensional faults. However, some subtle form of strike-slip fault characteristics are typically present,

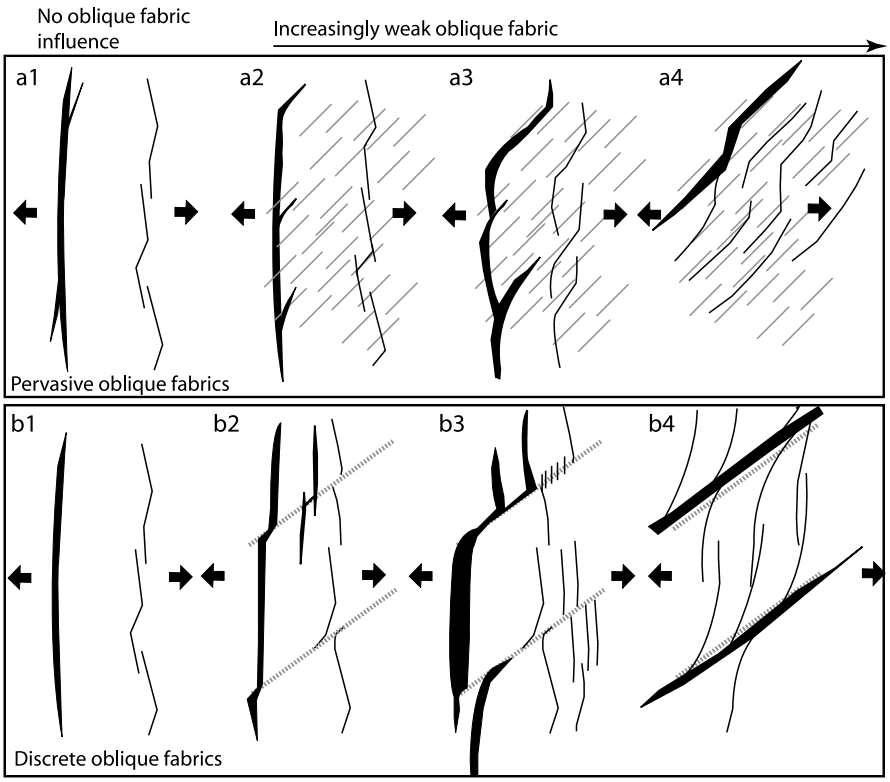

Fig. 17. Schematic plan view illustration of how extensional fault patterns may change depending upon the type of pre-existing strength anisotropy (pervasive or discrete) and the relative weakness of the strength anisotropy. Slip tendency analysis indicates oblique fabrics will tend to become less influential (reactivate less) with decreasing values of α. However, the angle of oblique extension is not the only factor in influencing the character of oblique extension zones. The type, spacing, and weakness of the oblique fabric are also important. For the same orientation of oblique fabric the character of the rift geometry can vary enormously.

in particular the component of strike-slip motion will become important in the overlap zones. In experimental models enhanced extension in the dextral right-stepping and sinistral left-stepping geometries led to breaching of relay ramps by arrays of oblique extensional faults (e.g. Clifton et al., 2000). Right-lateral left-stepping geometries and left-lateral right-stepping geometries have been observed in experimental models to affect whether the upper or lower ramp is breached (Crider, 2001). Minor thrust and fold features can occur at compressional stepping geometries (sinistral right-stepping, dextral left-stepping; Figs. 10 and 18). (2) Oblique-striking fault segments and releasing bend geometries are likely to be sites of depocentre thicks (Fig. 10). Without strain partitioning restraining bend compressional deformation is unlikely to develop. Fault segments that lie at a relatively low-angle to the regional displacement direction will display lower throw (i.e. lower subsidence) and a larger strike-slip component of motion (Fig. 18). (3) Basins will develop in the hanging wall similar to pure extensional faults; however, there may be an asymmetry to the basin geometry, reflecting the presence of compressional and extensional fault tips due to the oblique motion (Fig. 10). Unfortunately this may be difficult to distinguish from asymmetries developed along segmented pure dip-slip normal faults. (4) Secondary faults are more likely to follow extensional fault patterns than strike-slip faults, given the small strike-slip component. Very commonly in oblique settings, faults are either parallel to the basement fabric, or perpendicular to the regional extension direction (e.g. Figs. 4–6, 9 and 13). This is the typical pattern produced in experimental models. Hence a distinctive bi-directional character to splays and secondary faults is a common feature of oblique extension. The two fault orientations can lead to a distinctive sigmoidal-shape to faults near oblique trends where faults curve from the rift oblique to the rift parallel trends (Le Turdu et al., 1999; Kornsawan and Morley, 2002; Fig. 18).

11. Describing oblique fault populations

The western part of the Mae Moh mine (Fig. 7) is characterised by numerous faults either linking with or intersecting each other. The mass of touching or nearly touching faults presents a problem for description of fault populations by measurement of cumulative frequency, fault length and displacement amount. Fault linkage in three dimensions is likely to be considerably greater than even the 2D map images suggest. In many cases fault length is defined because at the point of linkage with another fault segment displacements are very low and fault strike-directions are different. However, such criteria are rather

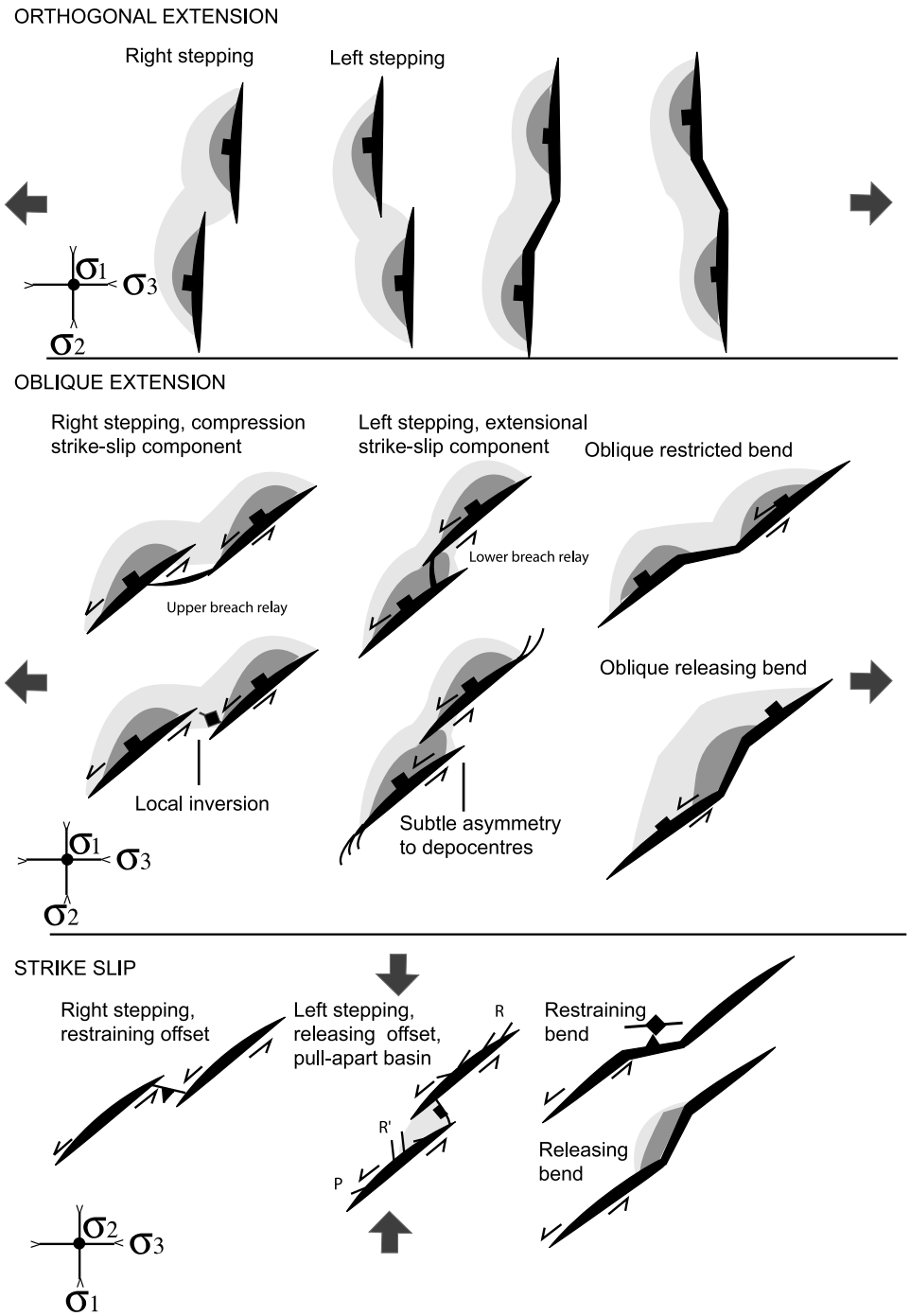

Fig. 18. Comparison of how similar, commonly occurring fault geometries (en échelon synthetic faults, zig-zag bends) developed under extension, oblique slip and strike-slip will differ in terms of depocentre geometry and development of secondary structures. In particular, structures and depocentre locations found at releasing–restraining bend geometries and en-échelon relay geometries can be critical in determining the style of deformation.

arbitrary. In Fig. 12 the Bongkot area shows linkage of up to seven faults.

To quantify how fault length is influenced by the degree of oblique extension Clifton et al. (2000) used tortuosity, which is the measured length (*m*l) along the fault/tip-to-tip fault length (*t*l). This method takes into account the length of the fault including its splays, but not the number of splays. An important aspect of pre-existing fabric influence is the number of splays that branch off a fault. Splays are not necessarily low-displacement secondary features. In the case of the Bongkot area, the longest fault segment (NW–SE strike) actually represents linked, low-displacement fault tips, whereas the 'splays' (N–S strike) actually are the highest displacement parts of the fault zone (Figs. 12 and 16a). Splays can be quantified as the average occurrence of fault segments between splays per unit fault length (fault

splay spacing, FSS) (expressed as a fraction of one because one equals a single non-branching fault). Using (*tl*/*ml*) where the measured fault length includes all splays, a tortuous fault will be expressed as a fraction, with a single straight fault having a maximum value of one. A more complete numerical discrimination of the effects of fault splays on fault length is given by:

$$(tl/ml) \times \mathrm{FSS} = \text{Fault Branch Factor (FBF)}$$

Hence a single straight fault FBF = 1. As a fault becomes increasingly tortuous, with more splays it is represented by an increasingly smaller fraction.

It is also apparent from Figs. 13 and 15 that fault length is important when describing oblique fault characteristics. For example in Figs. 12, 13 and 15 there is a population of long tortuous faults and a population of shorter less tortuous faults, with fewer splays and linkage geometries. To identify these populations normalised fault length expressed as a percentage of the total fault population length can be plotted against fault tortuosity, fault splay spacing, or FBF (Fig. 19). For the Pattani Basin examples the syn-rift faults show a mixture of short and long, low tortuosity faults and medium to long high tortuosity faults. The post-rift faults show a greater segregation into short, low tortuosity faults and long, high tortuosity faults. As illustrated in Figs. 13 and 15 this segregation reflects the strong control of long syn-rift faults on the longest faults in the post-rift section. As long oblique faults develop and link with shorter extension-orthogonal faults and become more dominant there will be a tendency for the fault population to show deviation from the typical fault length–displacement and fault cumulative frequency–displacement relationships. The long oblique faults plot to the right of 'typical' fault population trends on fault length–displacement graphs, since the long-oblique faults show less displacement than would typically be characteristic for their length (Fig. 12c). For graphs of fault cumulative frequency vs. displacement, the high cumulative frequency, lower displacement region of fault populations will become depopulated as shorter, lower displacement faults become linked with the long oblique trends (Fig. 12d).

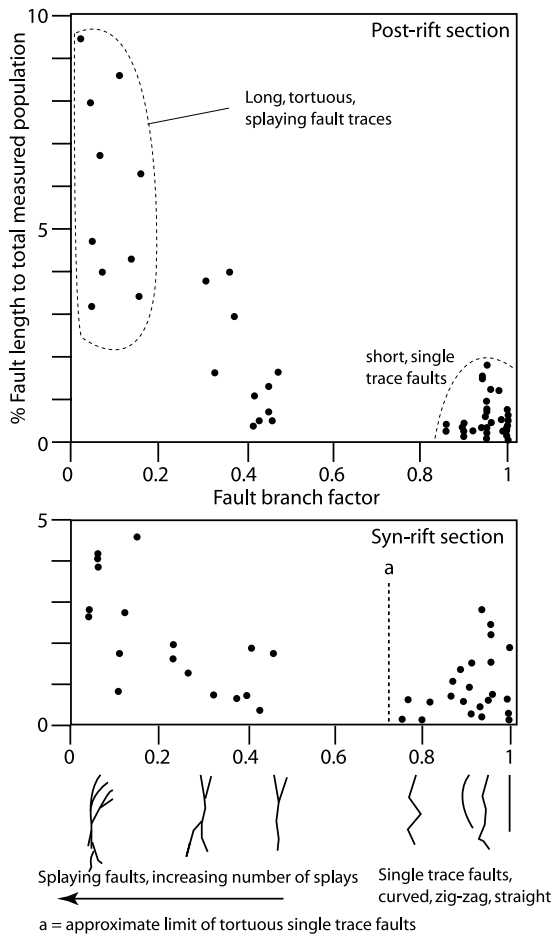

Fig. 19. Graphs of fault length as a percentage of the total length of the fault population vs. fault branch factor, for syn-rift and fault rift fault populations in the Pattani Basin described in this paper (Figs. 11, 13 and 14).

12. Conclusions

1. Extensional fault systems are influenced in a number of ways by oblique pre-existing fabrics including (1) oblique orientation of faults, (2) oblique fault splay geometries (Fig. 16), (3) the location, geometry and style of transfer zones (Figs. 17 and 18), and (4) fault linkage and displacement patterns.
2. The Uttardit fault demonstrates that, at high angles to the extension direction, oblique extensional faults can retain geometries that in general are similar to orthogonal extension half grabens. However, folds and thrusts at compressional fault tips and the location of depocentres at releasing bends are diagnostic characteristics.
3. Basins associated with oblique extension develop in the hanging walls of normal oblique slip faults very similar to pure extensional faults. Enhanced subsidence of basins may occur between en-échelon faults with an extensional stepping direction. Some asymmetry to the basin geometry is to be expected.
4. Many rifts in northern Thailand have undergone oblique extension. In areas like the western side of Mae Moh mine the fault geometries strongly resemble sandbox models for oblique extension ($\alpha = 45°$) (Withjack and Jamison, 1986). The oblique fault system is juxtaposed with an orthogonal extensional fault system. Whilst at the scale of Mae Moh mine the fault pattern resembles the experimental models (e.g. Clifton et al., 2000), the more regional fault pattern (Fig. 1) does not. This is because different types of pre-rift fabric exert influence at different scales. Extensional fault population characteristics such as fault displacement/length ratio, number of faults of a particular size, fault linkage patterns and fault tortuosity appear to be significantly changed when oblique fabrics play a significant role. These patterns can be regional or local, and will change depending upon the scale of the oblique fabric. Hence, fault populations

in rifts strongly influenced by pre-rift fabrics should not be expected to behave as a single fractal population.

5. The degree of oblique opening is just one factor that influences the way oblique fabrics develop; however, this is the factor that is emphasised in sandbox models. Equally, if not more important is the number, relative strength, dip, strike, spacing, and type (pervasive or discrete) of fabric element. There is tremendous variety to the types of oblique fabric geometries that can develop. Changes in oblique fabric character can cause abrupt changes in structural style. For example in the Mae Moh mine an orthogonal extensional fault system is juxtaposed to a fault system possessing a strongly oblique character.
6. Caution is necessary when interpreting the palaeostress history of oblique extension because of potential multiple causes of the fault patterns including: (a) rotation of stress field with time, (b) local features such as basement blocks and fault tips causing local rotation of stresses (Fig. 16b and c), (c) varying the ratio of the intermediate principal stress with respect to the other two principal stresses, and (d) evolving failure criteria favouring the early development of oblique fabrics (Coulomb failure criteria, anisotropic rock strength), whilst once the faults are established, the sliding friction criteria favours continued activation of more optimally oriented faults (Figs. 3 and 4). However, the way oblique faults are activated through time also provides an important way of accessing paleostress information.

Acknowledgements

We thank Unocal Thailand, Shell Thailand, PTTEP and the Electricity Generating Authority of Thailand for providing the data and logistical help, and the Universiti of Brunei Darussalam for funding the work. Very helpful, detailed and constructive reviews were provided by Chuck Kluth and Roy Schlische and, for an earlier version of the manuscript, by Greg Solomon and Anuroj Napattaloong. Thanks to Mark Tingay for producing the FAST plots in Fig. 4.

References

Anderson, E.M., 1951. The Dynamics of Faulting, 2nd ed, Oliver and Boyd, Edinburgh.

Angelier, J., Tarantola, A., Valette, B., 1982. Inversion of field data in fault tectonics to obtain the regional stress—1. Single phase fault populations: a new method of computing the stress tensor. Geophysical Journal of the Royal Astronomical Society 69, 607–621.

Bal, A.A., Burgisser, H.M., Harris, D.K., Herber, M.A., Rigby, S.M., Thumprasertwong, S., Winkler, F.J., 1992. The Tertiary Phitsanulok lacustrine basin, Thailand. Geological Resources of Thailand: Potential for Future Development. Department of Mineral Resources, Bangkok, November, 1992, pp. 247–258.

Bonini, M., Souriot, T., Boccaletti, M., Brun, J.P., 1997. Successive orthogonal and oblique extension episodes in a rift zone: laboratory experiments with application to the Ethiopian Rift. Tectonics 16, 347–362.

Bott, J., Wong, I., Prachuab, S., Wechbunthung, B., Hinthong, C., Surapirome, S., 1997. Contemporary seismicity in northern Thailand and its tectonic implications. The International Conference on Stratigraphy and Tectonic Evolution of Southeast Asia and the South Pacific, Bangkok, Thailand. Department of Mineral Resources, pp. 453–464.

Bott, M.P.H., 1959. The mechanics of oblique-slip faulting. Geological Magazine 96, 109–117.

Bustin, R.M., Chonchawalit, A., 1995. Formation and tectonic evolution of the Pattani Basin, Gulf of Thailand. International Geology Review 37, 866–892.

Byerlee, J.D., 1978. Friction of rocks. Pure Applied Geophysics 116, 615–626.

Carey, E., 1979. Recherce des directions principales de contraintes associees au jeu d'une population des failles. Review Geology Dynamics Geography and Physics 21, 57–66.

Chang, C., Haimson, B., 2000. True triaxial strength and deformability of the German Continental Deep Drilling Program (KTB) deep hole amphibolite. Journal of Geophysical Research 105, 18,999–19,013.

Clifton, A.E., Schlische, R.W., Withjack, M.O., Ackermann, R.V., 2000. Influence on rift obliquity on fault-population systematics: results of experimental clay models. Journal of Structural Geology 22, 1491–1509.

Crider, J.G., 2001. Oblique slip and the geometry of normal-fault linkage: mechanics and a case study from the Basin and Range in Oregon. Journal of Structural Geology 23, 1997–2009.

Cullen, P.J., Birch, P.L., Wright, S.C., Kearney, C.J., Pink, A.T., 1997. Exploration in the Savannakhet basin, Peoples Democratic Republic of Laos. Indonesian Petroleum Association Proceedings, Jakarta, Indonesia, pp. 425–447.

Daily, M.C., Chorowicz, J., Fairhead, D., 1989. Rift basin evolution in Africa: the influence of reactivated steep basement shear zones. In: Cooper, M.A., Williams, G.D. (Eds.), Inversion Tectonics, Geological Society of London Special Publication, 44., pp. 309–334.

Department of Mineral Resources, 2001, Geological Map of Thailand, 1:1,000,000, Department of Mineral Resources, Bangkok, Thailand.

Dewey, J.F., Holdsworth, R.E., Strachan, R.A., 1998. Transpression and transtension zones. In: Holdsworth, R.E., Strachan, R.A., Dewey, J.F. (Eds.), Continental Transpressional and Transtensional Tectonics, Geological Society, London, Special Publication, 135., pp. 1–14.

Dixon, T.H., Stern, R.J., Hussein, I.M., 1987. Control of Red Sea rift geometry by Precambrian structures. Tectonics 6, 551–571.

Fenton, C.H., Charusiri, P., Hinthong, C., Lumjuan, A., Mangkonkarn, B., 1997. Late Quaternary faulting in northern Thailand. The International Conference on Stratigraphy and Tectonic Evolution of Southeast Asia and the South Pacific, Bangkok, Thailand, pp. 436–452.

Flint, S., Stewart, D.J., Hyde, T., Gevers, C.A., Dubrule, O.R.F., Van Riessen, E.D., 1988. Aspects of reservoir geology and production behaviour of Sirikit Oil Field, Thailand: an integrated study using well and 3-D seismic data. American Association of Petroleum Geology Bulletin 72, 1254–1268.

Fossen, H., Tikoff, B., 1993. The deformation matrix for simultaneous simple shearing, pure shearing and volume change, and its application to transpression/transtension tectonics. Journal of Structural Geology 15, 423–432.

Haimson, B., Chang, C., 2000. A new true triaxial cell for testing mechanical properties of rock, and its use to determine rock strength and deformability of Westerly granite. International Journal of Rock Mechanics and Mining Sciences 37, 285–296.

Harrison, T.M., Leloup, P.H., Ryerson, F.J., Tapponier, P., Lacassin, R., Chen, W., 1996. Diachronous initiation of transtension along the Ailao Shan-Red River shear zone, Yunnan and Vietnam. In: Yin, A., Harrison, M.T. (Eds.), The Tectonic Evolution of Asia, Cambridge University Press, Cambridge, pp. 208–226.

Higgins, R.I., Harris, L.B., 1997. The effect of cover composition on

extensional faulting above re-activated basement faults; results from analog modelling. Journal of Structural Geology 19, 89–98.
Horsfield, W.T., 1980. Contemporaneous movement along crossing conjugate normal faults. Journal of Structural Geology 2, 305–310.
Huchon, P., Le Pichon, X., Rangin, C., 1994. Indo-China Peninsular and the collision of India and Eurasia. Geology 22, 27–30.
Jaeger, J.C., Cook, N.G.W., 1967. Fundamentals of Rock Mechanics, Halstead Press, New York, 585pp.
Jardine, E., 1997. Dual petroleum systems governing the prolific Pattani basin, offshore Thailand. Petroleum Systems of S.E. Asia and Australasia Conference, Jakarta, May 21–23, 1997, pp. 351–363.
Jones, R.M., Boult, P., Hillis, R.R., Mildren, S.D., Kaldi, J., 2000. Integrated hydrocarbon seal evaluation in the Penola Trough, Otway Basin. Australian Petroleum, Production & Exploration Association Journal, 194–212.
Keep, M., McClay, K.R., 1997. 3D analogue modelling of multiphase rift systems. Tectonophysics 273, 239–270.
Knox, G.J., Wakefield, L.L., 1983. An Introduction to the Geology of the Phitsanulok Basin. Conference on Geology and Mineral Resources of Thailand, Bangkok, 19–28 November, 9pp.
Kong, X., Bird, P., 1996. Neotectonics of Asia: thin-shell finite-element models with faults. In: Yin, A., Harrison, M.T. (Eds.), The Tectonic Evolution of Asia, Cambridge University Press, Cambridge, pp. 18–34.
Kornsawan, A., Morley, C.K., 2002. The origin and evolution of complex transfer zones (graben shifts) in conjugate fault systems around the Funan Field, Pattani basin, Gulf of Thailand. Journal of Structural Geology 24, 435–449.
Lacassin, R., Hinthong, C., Siribhakdi, K., Chauviroj, S., Charoenravat, A., Maluski, H., Leloup, P.H., Tapponnier, P., 1997. Tertiary diachronic extrusion and deformation of western Indochina: structure and $^{40}Ar/^{39}Ar$ evidence from NW Thailand. Journal of Geophysical Research 102(B5), 10013–10037.
Leloup, P.H., Arnaud, N., Lacassin, R., Kienast, J.R., Harrison, T.M., Trong, T.T.P., Replumaz, A., Tapponnier, P., 2001. New constraints on the structure, thermochronology and timing of the Ailao Shan–Red River shear zone, SE Asia. Journal of Geophysical Research 106, 6683–6732.
Le Turdu, C., Tiercelin, J.-J., Richert, J.-P., Rolet, J., Xavier, X.-P., Renaut, R.W., Lezzar, K.E., Coussement, C., 1999. Influence of pre-existing oblique discontinuities on the geometry and evolution of extensional fault patterns: evidence from the Kenya rift using SPOT imagery. In: Morley, C.K., (Ed.), Geoscience of Rift Systems—Evolution of East Africa, American Association of Petroleum Geologists Studies in Geology, 44., pp. 173–191.
Lockhart, B.E., Chinoroje, O., Enomoto, C.B., Hollomon, G.A., 1997. Early Tertiary deposition in the southern Pattani Trough, Gulf of Thailand. The International Conference on Stratigraphy and Tectonic Evolution of Southeast Asia and the South Pacific, Bangkok, Thailand, pp. 476–489.
Macdonald, A.S., Barr, S.M., 1984. The Nan River mafic–ultramafic belt, northern Thailand: geochemistry and tectonic significance. Bulletin of the Geological Society of Malaysia 17, 209–217.
McClay, K.R., White, M., 1995. Analogue models of orthogonal and oblique rifting. Marine and Petroleum Geology 12, 137–151.
McClay, K.R., Dooley, T., Whitehouse, P., Mills, M., 2002. 4-D evolution of rift systems: insights from scaled physical models. American Association of Petroleum Geologists Bulletin 86, 935–960.
McConnell, R.B., 1972. Geological development of the rift system of eastern Africa. Geological Society of America Bulletin 83, 2549–2572.
Meyer, J.J., 2002. The determination and application of in situ stresses in petroleum exploration and production. Ph.D. Thesis, University of Adelaide, Australia.
Mildren, S.D., Hillis, R.R., Kaldi, J., 2002. Calibrating predictions of fault seal reactivation in the Timor Sea. Australian Petroleum, Production & Exploration Association Journal, 187–202.
Morley, C.K., 1995. Developments in the structural geology of rifts over the last decade and their impact on hydrocarbon exploration. In: Lambiase, J., (Ed.), Hydrocarbon habitat of rift basins, Geological Society of London Special Publication, 80., pp. 1–32.
Morley, C.K., 1999. How successful are analogue models in addressing the influence of pre-existing fabrics on rift structure? Journal of Structural Geology 21, 1267–1274.
Morley, C.K., 2001. Combined escape tectonics and subduction rollback-back arc extension: a model for the evolution of Tertiary rift basins in Thailand, Malaysia and Laos. Journal of the Geological Society of London 158, 461–474.
Morley, C.K., Wonganan, N., 2000. Normal fault displacement characteristics, with particular reference to synthetic transfer zones, Mae Moh Mine, Northern Thailand. Basin Research 12, 1–22.
Morley, C.K., Cunningham, S.M., Wescott, W.A., Harper, R.M., 1992. Geology and geophysics of the Rukwa rift, East Africa. Tectonics 11, 69–81.
Morley, C.K., Sangkumarn, N., Hoon, T.B., Chonglakmani, C., Lambiase, J., 2000. Structural evolution of the Li Basin northern Thailand. Journal of the Geological Society of London 157, 483–492.
Morley, C.K., Woganan, N., Sankumarn, N., Hoon, T.B., Alief, A., Simmons, M., 2001. Late Oligocene–Recent stress evolution in rift basins of Northern and Central Thailand: implications for escape tectonics. Tectonophysics 334, 115–150.
Morris, A.P., Ferrill, D.A., Henderson, D.B., 1996. Slip-tendency analysis and fault reactivation. Geology 24, 275–278.
Nicol, A., Walsh, J.J., Watterson, J., Bretan, P.G., 1995. Three dimensional geometry and growth of conjugate normal faults. Journal of Structural Geology 17, 847–862.
O'Leary, H., Hill, G.S., 1989. Tertiary basin development in the Southern Central Plains, Thailand. Proceeding of the International Conference on Geology and Mineral Resources of Thailand, Bangkok, pp. 1–8.
Polachan, S., Pradidtan, S., Tongtaow, C., Janmaha, S., Intarawijitr, K., Sangsuwan, C., 1991. Development of Cenozoic basins in Thailand. Marine and Petroleum Geology 8, 84–97.
Ranalli, G., Yin, Z.M., 1990. Critical stress difference and orientation of faults in rocks with strength anisotropies: the two dimensional case. Journal of Structural Geology 12, 1067–1071.
Rhodes, B.P., Blum, J., Devine, T., Ruangvataasirikul, K., 1997. Geology of the Doi Suthep metamorphic complex and adjacent Chiang Mai Basin. Proceedings of the International Conference on Stratigraphy and Tectonic Evolution in Southeast Asia and the South Pacific, Bangkok, Thailand, pp. 305–313.
Rhodes, B.P., Perez, R., Lamjuan, A., Kosuwan, S., 2002. Kinematics of the Mae Kuang Fault, Northern Thailand Basin and Range Province. The Symposium on Geology of Thailand, Bangkok Thailand, August 2002, pp. 298–308.
Rigo de Rhigi, L., Baranowski, J., Chaikiturajai, C., Nelson, G., Wechsler, D., Mattingly, G., 2002. Bolck B8/32, Gulf of Thailand Petroleum System and Implementation of Technology in Field Development. Seapex Press 6, pp. 46–55.
Ring, U., 1994. The influence of preexisting structure on the evolution of the Cenozoic Malawi Rift (East African Rift System). Tectonics 13, 313–326.
Ronghe, S., Surarat, K., 2002. Acoustic impedance interpretation for sand distribution adjacent to a rift boundary fault, Suphan Buri basin, Thailand. American Association of Petroleum Geologists Bulletin 86, 1753–1771.
Sanderson, D., Marchini, R.D., 1984. Transpression. Journal of Structural Geology 6, 449–458.
Schlische, R.W., Withjack, M.O., Eisenstadt, G., 2002. An experimental study of the secondary deformation produced by oblique-slip normal faulting. American Association of Petroleum Geologists Bulletin 86, 885–906.
Schreurs, G., Colletta, B., 1998. Analogue modelling of faulting in zones of continental transpression and transtension. In: Holdsworth, R.E., Strachan, R.A., Dewey, J.F. (eds.), Continental Transpressional and Transtensional Tectonics, Geological Society of London Special Publication, 135, 59–79.

Sibson, R., 1977. Fault rocks and fault mechanisms. Journal of the Geological Society of London 133, 191–214.

Singharajwarapan, S., Berry, R.F., 1993. Structural analysis of the accretionary complex in Sirikit Dam area, Uttaradit, Northern Thailand. Journal of Southeastern Asian Earth Sciences 8, 233–245.

Smith, M., Mosley, P., 1993. Crustal heterogeneity and basement influence on the development of the Kenya Rift, East Africa. Tectonics 12, 591–606.

Sylvester, A.G., 1988. Strike-slip faults. Geological Society of America Bulletin 100, 1669–1703.

Tapponnier, P., Peltzer, G., Armijo, R., 1986. On the mechanism of collision between India and Asia. In: Coward, M.P., Ries, A.C. (Eds.), Collision Tectonics, Geological Society of London Special Publication, 19., pp. 115–157.

Tron, V., Brun, J.P., 1991. Experiments on oblique rifting in brittle–ductile systems. Tectonophysics 188, 71–84.

Watterson, J., Nicole, A., Walsh, J.J., Meier, D., 1998. Strain at the intersection of synchronous conjugate normal faults. Journal of Structural Geology 20, 363–370.

Withjack, M.O., Jamison, W.R., 1986. Deformation produced by oblique rifting. Tectonophysics 126, 99–124.

Woodcock, N.H., Schubert, C., 1994. Continental strike-slip tectonics. In: Hancock, P.L., (Ed.), Continental Deformation, Pergamon Press, Oxford, pp. 251–263.

Yale, D.P., Rodriguez, J.M., Mercer, T.B., Blaisdell, D.W., 1994. In-situ stress orientation and the effects of local structure—Scott Field, North Sea. In: Eurock '94, Proceedings of the 1994 Eurock Conference, Delft, August, 1994, Balkema, Rotterdam, pp. 945–951.

Youash, Y., 1969. Tension tests in layered rocks. Geological Society of America 80, 303–306.